ELSEVIER

Journal of Structural Geology 28 (2006) 333–352

JOURNAL OF STRUCTURAL GEOLOGY

www.elsevier.com/locate/jsg

The development and behaviour of low-angle normal faults during Cenozoic asymmetric extension in the Northern Apennines, Italy

C. Collettini [a,*], N. De Paola [a,b], R.E. Holdsworth [b], M.R. Barchi [a]

[a] *Geologia Strutturale Geofisica, Dipartimento di Scienze della Terra Università di Perugia, Perugia, Italy*
[b] *Department of Earth Sciences, Reactivation Research Group, University of Durham, Durham DH1 3LE, UK*

Received 20 December 2004; received in revised form 15 July 2005; accepted 4 October 2005
Available online 14 November 2005

Abstract

Movements on low-angle normal faults (LANF) are not predicted by traditional Anderson–Byerlee frictional fault mechanics. Our investigations centre on three normal fault systems active at distinct times during the regional extension of the Northern Apennines, with each showing different degrees of crustal exhumation. These are (from E to W): the Altotiberina fault system, Umbria; the Radicofani fault system, Tuscan mainland; and the Zuccale fault system, Isle of Elba. Regional extension has been a continuous process since middle Miocene, migrating progressively from west to east, with deformation accommodated by a set of E to NE-dipping LANF and more steeply SW-dipping antithetic structures. The LANF acted as regional detachments, accommodating a majority of the extension in the Northern Apennines, with individual faults exhibiting several kilometres of displacement. Regionally, the stress field has been characterised by a vertical σ_1 and a NE–SW- (Tuscan mainland and Umbria) to E–W (Elba)-trending σ_3. Where exposed at the surface, the main LANF detachments possess a well-developed fault core of foliated fault rocks in which fluids have played a key role in weakening due to reaction softening and the onset of stress-induced solution–precipitation mechanisms. We speculate that the E-dipping normal faults initiated with relatively low-angles of dip due to differential drag generated by mantle flow following slab retreat and roll-back beneath the Apennine chain.

Keywords: Northern Apennines; Normal faults; Reactivation; Earthquakes

1. Introduction: the mechanical paradox of LANF

The mechanics of low-angle normal faults (LANFs) is a controversial topic in scientific literature. According to classical Anderson–Byerlee frictional fault mechanics, an extending region characterised by vertical trajectories of σ_1 and faults possessing Byerlee's friction coefficients ($0.6 < \mu_s < 0.85$), should contain normal faults in the brittle upper crust that initiate at $\sim 60°$ and rotate down to 30° while active (e.g. Sibson, 1985). Normal faults may then be further reoriented passively as inactive structures to very low angles either due to rotation during later episodes of normal faulting along new, steeply dipping structures (Proffett, 1977), or due to isostatic adjustments (Wernicke and Axen, 1988). This mechanical theory is consistent with the observed dip-range of moderate and large normal-slip ruptures identified using positively discriminated focal mechanisms: the dip-distribution extends from 30 to 65°, with no unambiguous examples of $M > 5.5$ earthquakes on faults dipping less than 30° (Jackson and White, 1989; Collettini and Sibson, 2001, but see also Axen, 1992, 1999; Wernicke, 1995). Some authors have proposed different mechanical theories in which stress rotations occur either due to changes in the rheology as one moves from the elastic upper crust into the viscous lower crust (Lister and Davis, 1989; Melosh, 1990) or resulting from the action of subhorizontal shear stress at the base of the brittle upper crust (Yin, 1989; Westaway, 1999). Such stress tensor reorientation could then favour initiation and repeated reactivation of LANFs.

For structural geologists, a key question must be—are LANFs important structures for accommodating significant amounts of extension? If the answer is yes, how can we account for this behaviour? To address these issues we focus here on the Northern Apennines of Italy where extension within the brittle upper crust is accommodated by a set of

* Corresponding author. Tel./fax: +39 075 5852651.
E-mail address: colle@unipg.it (C. Collettini).

0191-8141/$ - see front matter © 2005 Elsevier Ltd. All rights reserved.
doi:10.1016/j.jsg.2005.10.003

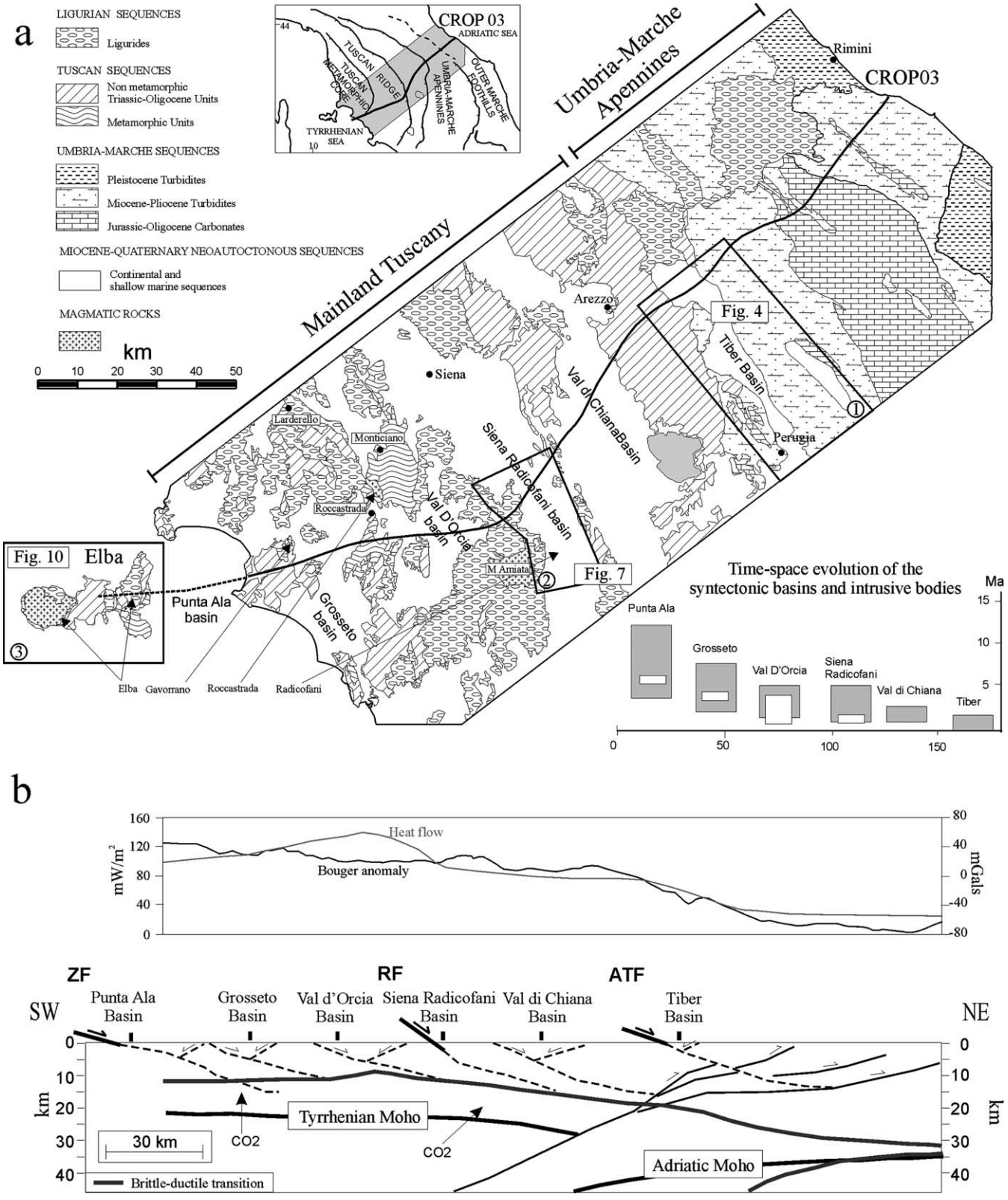

Fig. 1. (a) Location map of the CROP 03 seismic reflection profile and main geological units. Boxes show the three study areas located in the Umbria region (box 1 and Figs. 4–6), mainland Tuscany (box 2 and Figs. 7–9) and Isle of Elba (box 3 and Figs. 10–12). The time–space evolution of the syntectonic basins and magmatism is shown bottom left (modified from Collettini and Barchi, 2004). (b) Measured gravity anomalies and crustal-scale cross-section from Elba to the Adriatic coast based on the CROP03 deep seismic profile (Barchi et al., 1998). The profile shows that most of the extension is accommodated by upper-crustal, east-dipping LANF. The extensional processes in the Tyrrhenian Sea and Tuscany have been sufficient to cause exhumation, higher than average heat flows, a regional positive Bouguer gravity anomaly and a shallow Moho. The region also coincides almost exactly with a zone of anomalously high, deeply sourced CO_2 release. The depth to the brittle–ductile transition is also shown based on thermal modelling calibrated using surface heat flow measurements (after Pauselli and Federico, 2002).

major east-northeast dipping LANFs (Barchi et al., 1998; Decandia et al., 1998) and associated high-angle structures. In this region, the onset of extension migrated with time from the Tyrrhenian Sea in the west to the Umbria–Marche Apennines in the east (e.g. Elter et al., 1975; Barchi et al., 1998; Jolivet et al., 1998). Older parts of the extensional system are significantly exhumed due in part to the effects of extension and also to regional uplift. As a result, it is possible to examine normal faulting processes at different crustal depths in a single extensional system and to compare these geological data with the seismicity associated with the currently active part of the fault system. In the present study, the geometry of the extensional systems has been reconstructed using seismic reflection profiles and field-based geological data, whilst the kinematics of the structures has been investigated using structural geological observations and seismological data. Data comparison and analysis allow us to address four key issues: (1) whether movements occur on LANFs in an 'Andersonian' extensional stress field; (2) the importance of LANFs in accommodating significant amounts of regional extension; (3) the role of fluids in facilitating fault zone weakening; and (4) the initiation, reactivation and slip mechanisms of LANFs.

2. Geological and geophysical background

From the Oligocene to the present day, the Northern Apennines have experienced two phases of eastward migrating deformation: an early compression with eastward-directed thrusting and a later phase of extension (e.g. Elter et al., 1975). The effects of these deformation episodes can be appreciated by studying geological and geophysical data along a transect extending from the Isle of Elba to the Adriatic coast (Fig. 1). Along this transect, we have selected three key areas for study (Fig. 1): (1) the active Altotiberina fault system in Umbria; (2) the older Radicofani fault system, preserving ancient upper crustal fault geometries and basin-fill sedimentary rocks; and (3) the ancient and exhumed mid-crustal Zuccale fault system in the Isle of Elba. Crustal extension—which is still active in the inner region of the Umbria–Marche Apennines—everywhere disrupts structural architectures formed during the preceding compressional phase leading to the development of thinned, uplifted and extended crust across this part of Italy.

2.1. Main geological units

Four main regional tectonic units are recognised in the SW–NE transect (Fig. 1) extending from the Isle of Elba to the offshore Adriatic (e.g. Carmignani et al., 1994; Barchi et al., 1998): (1) *The Ligurian sequences (Ligurides)* are represented by Jurassic ophiolites and their Jurassic–early Cretaceous sedimentary cover, overlain by Cretaceous–Oligocene flysch sequences. The Ligurides preserve evidence of old oceanic crust emplaced eastward over Tuscan sequences in the late Oligocene (Principi and Treves, 1984). (2) *The Tuscan sequences* are divided into non-metamorphic Triassic–Oligocene sedimentary units and deeper metamorphic crustal units. The former are Upper Triassic–Oligocene marine carbonates and turbidites deformed in a stack of east-verging thrust sheets (Tuscan Nappe). The latter are late Carboniferous–Tertiary cover sequences and Palaeozoic units (Hercynian basement) that crop out on the Monticiano–Roccastrada ridge and in Elba (Fig. 1). (3) *The Umbria–Marche sequences* consist of sedimentary rocks deposited on a continental margin with basal late-Triassic evaporites, Liassic platform carbonates and Jurassic–Oligocene pelagic sequences. The top of the sequence is represented by Miocene–Pleistocene turbidites that become progressively younger toward the Adriatic coast in accord with the eastward migration of the compressional front. (4) *The Miocene–Quaternary neoautochthonous sequences* comprise marine and fluvio-lacustrine sediments that fill syntectonic basins, formed during the extensional phase.

The integration of detailed seismic profiles with stratigraphic data (e.g. Barchi et al., 1998; Jolivet et al., 1998; Pascucci et al., 1999; Collettini and Barchi, 2004) allows the continuous migration of the onset of extension with time from the Tyrrhenian Sea to the Umbria–Marche Apennines to be reconstructed (Fig. 1). In the following account, the extensional structures discussed are those responsible for the majority of fault displacements and basin formation, although it is recognised that more recent, minor phases of deformation are also present locally.

2.2. Magmatism

Most published papers relate the Neogene–Quaternary magmatism of the Northern Apennines to extensional tectonics, but the geodynamic interpretation of the magmatic activity is controversial (e.g. Peccerillo, 1985; Lavecchia and Stoppa, 1990; Serri et al., 1993) and beyond the scope of the present paper. The first intrusive event is represented by the Sisco lamproitic sill (15–13.5 Ma) in eastern Corsica. Along the study transect, magmatic pulses of known age are preserved in Elba at 8–5 Ma (see below) and in Tuscany (Gavorrano 4.4 Ma, Roccastrada 2.5–2.2 Ma, Radicofani 1.3 Ma, M. Amiata 0.3–0.2 Ma intrusions). For present purposes it is important to emphasise that: (1) the age of magmatism decreases progressively from west to east; (2) the magmatism is closely related in space and time to extensional deformation; (3) magmatic activity typically starts in the final stages of extension and continues for some million years in the same location (Fig. 1). In Umbria, where extension is relatively recent, magmatism is almost absent.

2.3. Crustal structure

The CROP03 NVR survey (CROsta Profonda Project Near Vertical Reflection; Pialli et al., 1998) provides a

regional context to examine the relationship between extensional deformation structures at different crustal depths. The acquisition of the CROP03 was integrated with a wide angle refraction survey (Deep Seismic Sounding or DSS) recording locations almost coincident with the reflection profile (De Franco et al., 1998). The results of the project have been published in a special issue of the Memorie della Società Geologica Italiana (Pialli et al., 1998), while more recent and conflicting interpretations are proposed in Finetti et al. (2001).

Following Barchi et al. (1998), the key observations from the CROP03 profile are as follows (see Fig. 1a and b):

(1) In Tuscany, integration of NVR and DSS profiles locate the Tuscan Moho at 8 s two-way travel-time (TWT), corresponding to a depth ranging from 20 to 25 km, gently deepening to the east. Below the Adriatic coast the Moho is located at 12 s TWT (~30 km), from there it gently dips to the west below the Umbria – Marche Apennines.
(2) From the inner sector of the Umbria – Marche Apennines to the Tyrrhenian coast, the upper crust is characterized by six sub-parallel, easterly dipping reflectors traceable down to a depth of about 5 s TWT. These alignments are thought to be the seismic expression of east-dipping LANFs that merge near the surface with the western margins of a series of extensional basins (Barchi et al., 1998; Decandia et al., 1998; Collettini and Barchi, 2004). The extensional syntectonic basins, infilled with continental to shallow marine deposits, are, from west to east: the Punta Ala; Grosseto; Val d'Orcia; Siena-Radicofani; Val di Chiana and Tiber basins (Fig. 1b).
(3) In Tuscany, extensional tectonics active since the middle Miocene have largely obliterated the previous compressional structures so that they cannot be recognized on seismic profiles. In contrast, compressional structures are still clearly preserved below the Umbria – Marche Apennines where extension has been active for a much shorter time period, about 3 Ma (Barchi et al., 1998).

2.4. Seismicity, active stress field and geodetic strain

In the Italian peninsula, the strongest historical and instrumental earthquakes occur along the axis of the Apenninic chain. In the Northern Apennines (Fig. 2), the majority of the earthquakes cluster below the Umbria–Marche Apennines and are located between 0 and 20 km depths. The strongest earthquakes, $5.0 < M < 6.0$, nucleate in the depth range of 6–12 km and possess extensional focal mechanisms. A few sub-crustal earthquakes with compressional focal mechanisms and maximum depths of 100 km are present and are interpreted to be related to the ongoing subduction (Selvaggi and Amato, 1992; Di Stefano et al., 1999). Small, $3 < M < 5$, shallow earthquakes located close to the Adriatic coast are mainly characterised by thrust and strike–slip focal mechanisms, whilst small shallow mainly extensional earthquakes occur widely throughout Tuscany.

The integration of earthquake focal mechanisms with borehole breakouts allows the present day stress field of the

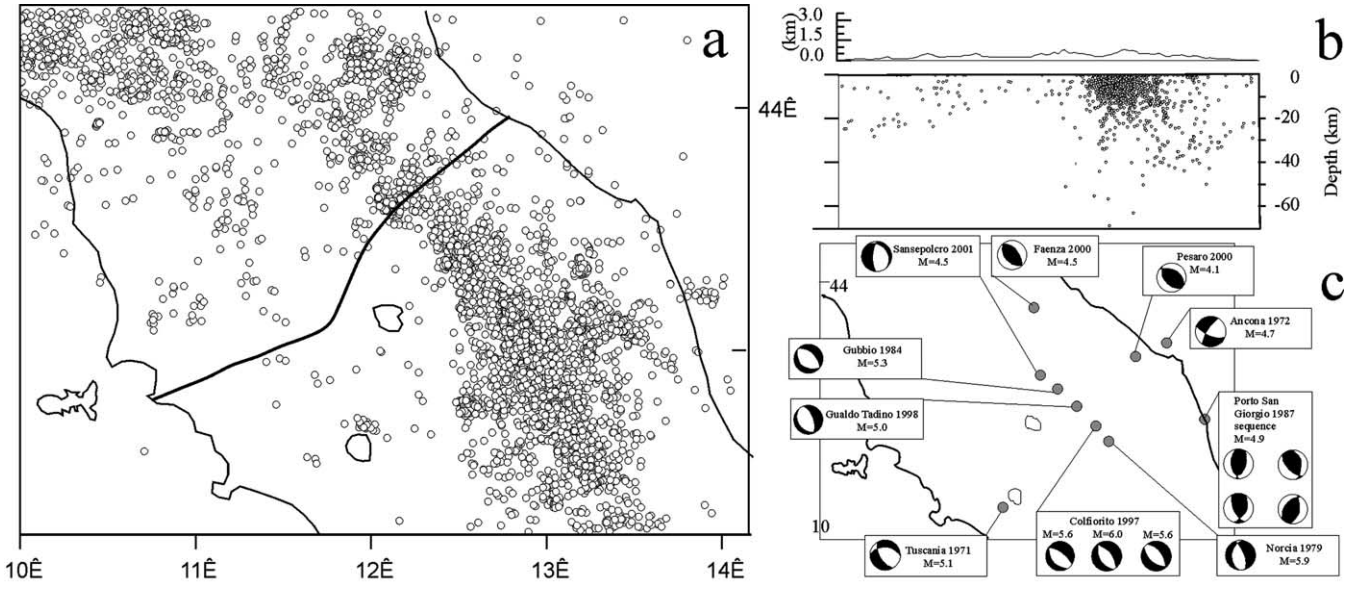

Fig. 2. Seismological data for the Northern Apennines. (a) Map of the seismicity ($M > 1.5$) during the 1981–2002 period (http://www.ingv.it/CSI/), solid line shows the trace of CROP03 seismic profile. (b) Hypocenter distribution along a section coinciding with the CROP03 seismic profile. (c) Distribution of the focal mechanisms with fault plane solutions: extensional events from Harvard CMT catalogue (www.seismology.harvard.edu) with the exception of Tuscania 1971 (Gasparini et al., 1985); Ancona 1972, strike–slip event (Gasparini et al., 1985); Porto San Giorgio 1987 sequence (Riguzzi et al., 1989); Pesaro 2000 (Borraccini et al., 2002); Faenza 2000 (Lavecchia et al., 2003).

Northern Apennines to be defined (Frepoli and Amato, 1997; Montone et al., 1999). In the Adriatic foreland (Fig. 3), the active stress field is not well constrained, although a direction of maximum extension is evident lying roughly parallel to the arcuate geometry of the Adriatic compressional front. In the inner sector of the Umbria–Marche Apennines, however, the active stress field is well defined with a direction of maximum extension oriented ~SW–NE. In Tuscany, the stress field is mainly characterised by ~SW–NE-trending extension, with more scattered regions of data corresponding to the locations of the Larderello and Monte Amiata geothermal fields (see Fig. 1).

Present-day extensional strain in the northern Apennines (Fig. 3) is concentrated across a 30–50-km-wide zone that coincides with the area where the strongest earthquakes occur (Hunstad et al., 2003), i.e. the Umbria region. Here, extension is oriented ~SW–NE, with rates of ~2.5 mm/year, increasing southeastwards to ~3.5 mm/year in agreement with the increment of the earthquake magnitudes. Relatively insignificant and heterogeneous deformation is observed in Tuscany.

2.5. Gravimetric, heat flow, mantle degassing

A gravimetric profile acquired along the CROP03 seismic profile (Marson et al., 1998) shows that the transect is divided into two distinct segments (Fig. 1b): from the Tyrrhenian coast to the Tiber basin, a long-wavelength positive Bouguer gravity anomaly (~30 mGals) is recorded, whilst a long-wavelength negative Bouguer gravity anomaly (~−80 mGals) characterises the Umbria–Marche Apennines further to the east. Short wavelength negative anomalies in Tuscany are thought to be caused by the infills of the Neogene extensional basins.

Heat flow values (Fig. 1b) are high in Tuscany (> 100 mW/m^2) with localised hot spots (>1000 mW/m^2) centring on the M. Amiata and Larderello geothermal fields (Mongelli and Zito, 1991). The flow values start to decrease close to the Tiber basin and reach a minimum value of 30 mW/m^2 below the Umbria–Marche chain.

The extended/extending sector of the Apennines (most of central and south Italy) is affected by a widespread and vigorous CO_2 degassing episode (Chiodini et al., 2004). Carbon mass balance calculations, relating aquifer geochemistry with dissolved inorganic carbon isotopic composition and hydrological data, have been used to determine the source(s) of CO_2 in the Apennines. Subordinate amounts come from the dissolution of crustal carbonates (33.2%) and from biogenic CO_2 in soils (23.5%), but the largest fraction (43.3%) derives from a deep mantle source (Chiodini et al., 2004). In the Northern Apennines, the CO_2-degassing crust extends from the Tyrrhenian Sea to the inner sector of the Umbria–Marche Apennines. The Adriatic sector (i.e. east of the location of the active extension) is not affected by deep CO_2 degassing (Chiodini et al., 2004). The boundary of the region where deep degassing processes are recognised corresponds closely to the area of active extension suggesting that deep fluids could play a key role in triggering seismicity (Collettini and Barchi, 2002; Chiodini et al., 2004; Miller et al., 2004).

2.6. Summary

The geological and geophysical data are consistent with the progressive migration of extension from the Tyrrhenian Sea to the Umbria–Marche Apennines from ca. 15 Ma to the present day (e.g. Elter et al., 1975). Active extension in the inner zone of the Umbria–Marche Apennines generates the largest earthquakes in the area and is responsible for an extension rate of 2.5 mm/year measured using geodetic techniques (Hunstad et al., 2003). Extension in the upper crust is contemporaneous with compression at depth and is thought to be consistent with subduction-related events (Selvaggi and Amato, 1992, but see also Lavecchia et al., 2003). In this area, the location of the Moho at 35 km depth, the low heat flow values and absence of magmatism suggest that crustal thinning is a relatively recent active process, not

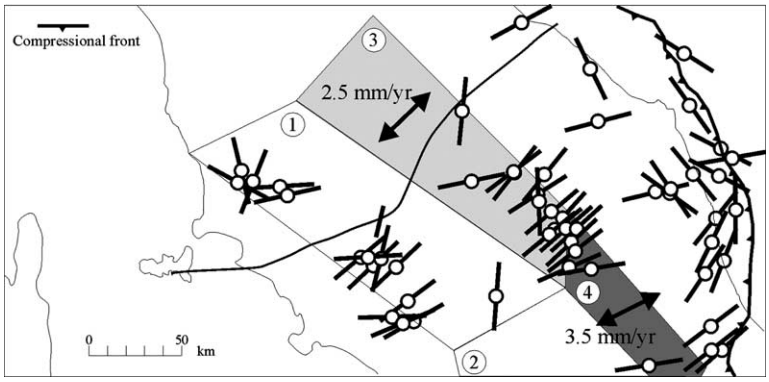

Fig. 3. Stress–strain map of the Northern Apennines. Bars with circles show orientation of the minimum horizontal stress (Montone et al., 1999; Mariucci and Muller, 2003). Extensional rates in central Italy shown for specific areas represented by polygons (data from Hunstad et al., 2003). NE–SW-trending extensional deformation is concentrated along the axis of the Northern Apennines (polygons 3 and 4), with only statistically insignificant and inhomogeneous deformation observed in polygons 1 and 2.

yet gone to completion. In contrast, extension in Tuscany has been active for enough time to change the geological and geophysical character of the area: the Moho is shallow, 20–25 km, heat flow is high and magmatism is widespread. The long-wavelength, positive Bouguer gravity anomaly results from the presence of a shallow, regional high-density body and has been interpreted to be either the top of the lithospheric mantle based on both passive seismology (e.g. Suhadolc and Panza, 1989) and thermal modelling (Pauselli and Federico, 2002) or as shallow new astenosphere (Peccerillo and Panza, 1999).

In addition to strongly influencing the geophysical data, the east-migrating extension has progressively exhumed the causative extensional structures. Therefore, the ancient structures exposed at the surface often provide clues as to what may be happening at depth in the currently active regions further to the east. In the following sections, we use well documented examples to focus on the architecture, geometry and kinematics of the extensional system at different depths.

3. The Altotiberina fault system, Umbria region

The Umbria region represents the actively extending part of the Umbria–Marche Apennines. The area is characterised by the presence of a complex pattern of thrusts, folds and normal faults, reflecting the superposition of the two main tectonic phases: an upper Miocene–lower Pliocene compressional phase, forming E–NE verging thrusts and folds, and a later upper Pliocene–Quaternary extensional phase, forming extensional basins bounded by normal faults (e.g. Barchi et al., 1998). The NNW–SSE-trending and 150-km-long alignment of SW-dipping normal faults, the Umbria Fault System (UFS) (Fig. 4), extending from Città di Castello as far south as Norcia, is thought to represent the active fault system of the Northern Apennines (e.g. Lavecchia et al., 1994; Barchi et al., 2000 and references therein). The Città di Castello segment has experienced some historical earthquakes (1458, MCS = IX; 1789, MCS = VIII–IX; 1917, MCS = IX), whilst the Gubbio area was affected in 1984 by a $M = 5.6$ event (Haessler et al.,

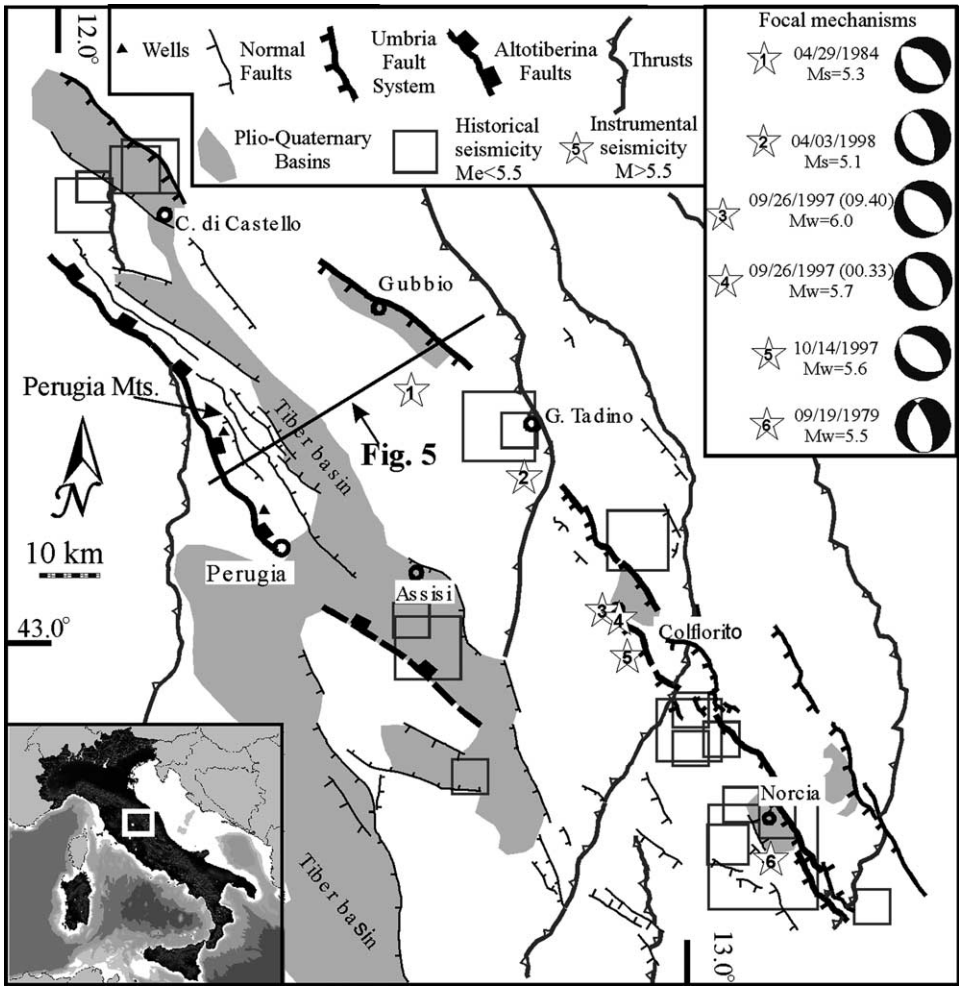

Fig. 4. Schematic structural map of Umbria showing the alignment of the intramountain basins (shaded) along the Umbrian Fault System. Historical seismicity is reported for the period 461 BC–1979 AD (Boschi et al., 1998). Focal mechanisms and magnitudes are for the 1997–1998 Colfiorito sequence (Ekström et al., 1998), for the 1979 Norcia earthquake (Deschamps et al., 1984), and for the 1984 Gubbio earthquake (Dziewonski et al., 1985). The trace of the cross-section in Fig. 5 is also shown.

1988). The Gualdo Tadino, Colfiorito and Norcia segments have been affected by both historical and instrumental seismicity. In particular, the Gualdo Tadino and Colfiorito areas were struck by a prolonged seismic sequence during 1997–1998 (Chiaraluce et al., 2003a) while the Norcia area recorded its last earthquake in 1979 (Deschamps et al., 1984).

3.1. Altotiberina fault system: architecture and kinematics

The CROP03 deep seismic reflection profile (Barchi et al., 1998 and Fig. 1) reveals the existence of a regional east-dipping low-angle normal fault, the Altotiberina Fault (ATF). The integration of surface geology with seismic reflection profiles, borehole and seismological data allow the geometry of the fault to be defined at depth (e.g. Barchi et al., 1999; Boncio et al., 2000; Collettini and Barchi, 2002; Piccinini et al., 2003; Mirabella et al., 2004). The surface expression of the ATF is represented by a splay of domino-like normal faults in the Perugia Mountains that detach downwards onto the ATF (Fig. 5). Structural analysis of striated fault planes (Boncio et al., 2000) depicts a prevailing NW–SE-trending fault alignment with dominant dip–slip movements. Subordinate right-lateral and left-lateral movements are observed, respectively, on E–W- and N–S-trending transfer faults. The inversion of the striated fault planes defines a stress tensor characterised by a near vertical σ_1 and NE-trending subhorizontal σ_3 (Boncio et al., 2000). The ATF is transected within two boreholes (see location in Fig. 4) where it emplaces Miocene turbidites over Triassic evaporites, omitting the intervening Umbria–Marche carbonates completely (Fig. 5). The easternmost splay of the ATF bounds the Tiber basin, which is infilled by Upper Pliocene Quaternary sediments (Ambrosetti et al., 1978). The asymmetrical shape of this basin is imaged clearly on the seismic reflection profiles and is consistent with movements along an eastward-dipping extensional fault. The age of the syntectonic sediments forming the Tiber basin and the displacement of the basin-bounding fault, ~2 km (Fig. 5), define a time-averaged long-term slip rate of ~1 mm/year over the last 2 Ma.

Good quality commercial seismic reflection datasets (Barchi et al., 1999; Collettini and Barchi, 2002; Mirabella et al., 2004) have been integrated with the CROP03 profile

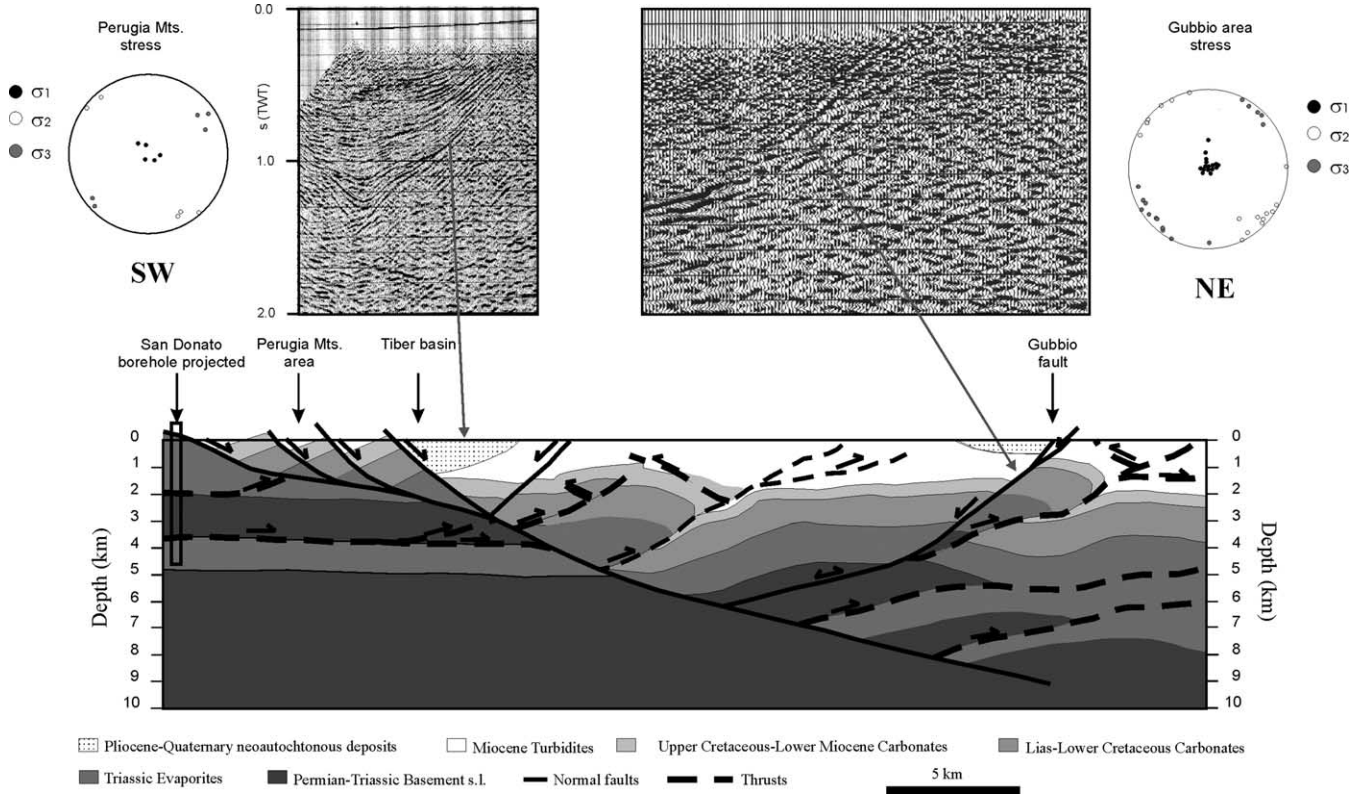

Fig. 5. Lower panel shows a geological cross-section through the Umbria Fault System (see location in Fig. 4). Data sources: surface observations in the Perugia Mts. (Minelli, 1992; Brozzetti, 1995); stratigraphy of the San Donato borehole (Anelli et al., 1994); subsurface interpretation derived from the integration of seismic refraction (Ponziani et al., 1995) and reflection surveys (Collettini and Barchi, 2002). The overlying insets show seismic reflection datasets that define the geometry of the syntectonic Tiber basin and the Gubbio normal fault. The asymmetrical shape of the upper Pliocene–Quaternary sediments infilling the basin is consistent with the activity of an east-dipping normal fault (left inset). The westward-dipping Gubbio normal fault is imaged by the westward-dipping alignment of the reflectors (right inset). The stereoplot (equal area projection, lower hemisphere) represents the orientation of the stress axis reconstructed at five structural stations in the Perugia Mts. (after Boncio et al., 2000) and at eight structural stations in the Gubbio area (Collettini et al., 2003).

in order to constrain the geometry of the ATF at depth and its relationship to the SW-dipping normal faults. The geometry of the ATF is highlighted by gently eastward-dipping alignments of the reflectors and the nearly flat attitude of the seismic markers in the ATF hanging wall that are abruptly truncated against the fault trace. Seismic reflection profiles allow the identification of the ATF from Città di Castello as far south as Perugia (an along-strike distance of ca. 60 km). The fault shows a nearly constant NNW–SSE direction and an average eastward dip of 20° (Fig. 5) with a total normal fault offset of 5–8 km (Collettini and Barchi, 2002). The hanging wall of the ATF is affected by an important antithetic SW-dipping normal fault, the Gubbio Fault, which is well exposed about 20 km east of the Tiber basin (Figs. 4 and 5). The Gubbio Fault at the surface is represented by a deformation zone (up to 150 m wide) consisting of synthetic and antithetic splays and a damage zone well-exposed in the footwall block. The inversion of slip data collected at different structural stations along the fault zone defines a stress tensor with a vertical σ_1 and a SW–NE oriented σ_3 (e.g. Boncio et al., 2000; Collettini et al., 2003).

3.2. Microseismic surveys

Two temporary microseismic networks were set up in the area between Perugia, Città di Castello and the Apenninic chain (Fig. 6): during May–June 1987, nearly 400 earthquakes with local magnitude ranging from 0.6 to 3.0 were recorded (Deschamps et al., 1989), whilst in the period October 2000–May 2001, more than 2200 earthquakes with local magnitude $M_L < 3.2$ occurred (Piccinini et al., 2003). The two surveys show similar characters (Fig. 6). Many microearthquakes are located close to the trace of the ATF as imaged by seismic reflection profiles and the magnitude of events is generally very small with peaks in the range 0.6–1.0. The time-evolution of the microseismicity is continuous (Piccinini et al., 2003), with the fault separating an active hanging wall from an almost aseismic footwall. The majority of focal mechanisms show extensional kinematics with NNW–SSE-trending nodal planes (Boncio et al., 2000; Piccinini et al., 2003) that are consistent with both geological structures mapped at the surface and highlighted by seismic reflection profiles. Inversion of the focal mechanisms (Boncio et al., 1996; Chiaraluce et al., 2003b) yields a stress tensor with a vertical σ_1 and a NE-trending subhorizontal σ_3. This stress tensor is consistent with the presently active stress field of the area (Montone et al., 1999; Chiaraluce et al., 2003a) and with the Quaternary geological stress field (Lavecchia et al., 1994; Boncio et al., 2000; Collettini et al., 2003).

The presence of relatively few gently eastward dipping nodal planes does not necessarily lessen the seismogenic role of the fault. As a result of the very low magnitude of the earthquakes, it is difficult to work out well-constrained focal mechanism solutions and those available only account for ~5% of the recorded seismicity. In our opinion, the alignment of a great number of microearthquakes along the ATF trace strongly supports fault activity along this low-angle structure. Finally, it is important to note that the gently eastward-dipping alignment of the seismicity, from 3 km depth below the Tiber valley down to 15 km below the Apenninic chain, does not correspond with the brittle–ductile transition that is thought to lie at greater depths based on models derived from heat flow data in the area (Pauselli and Federico, 2002). The present day picture of extension in the Northern Apennines—highlighted by the integration of geological and seismological data—depicts an extension driven by an east-dipping low-angle normal fault and antithetic structures. Both high-angle and low-angle normal faults accommodate deformation in a stress field characterised by a vertical σ_1.

4. The Radicofani fault system, mainland Tuscany

In the Siena-Radicofani area (Fig. 7a), compression was active during late Oligocene (Carmignani et al., 1994) forming a thrust stack topped by Ligurian units that overlie the Tuscan non-metamorphic sequence. The Tuscan units are internally subdivided into 1.5 km of basal Triassic evaporites (Burano Formation) overlain by ~2 km of Mesozoic carbonate sequence, followed by 2–3 km of upper Oligocene–Miocene foredeep flysch sediments. The extensional phase acted from late Miocene to late Pliocene forming the Siena-Radicofani Basin (Liotta and Salvatorini, 1994; Keller et al., 1996; Decandia et al., 1998; Barchi et al., 1998). In a different interpretation, the basin development has been related to the compressional rather than extensional regime (e.g. Bonini and Sani, 2002 and references therein). A detailed discussion as to whether the Siena-Radicofani Basin is compression or extension related is beyond the scope of the present paper, but our data support an extensional origin.

4.1. Geometry of the fault system at depth

Seismic reflection profiles crossing the Siena-Radicofani Basin highlight the shallow geometry (0–3 km) of the extensional fault system, represented by an east-dipping fault, the Radicofani Fault (RF), cropping out at the western margin of the basin, and the west-dipping Cetona Fault (CF), bounding the eastern side of the basin (Liotta and Salvatorini, 1994; Keller et al., 1994; Barchi et al., 1998).

The resolution of commercial seismic reflection profiles does not allow the identification of the extensional fault system at depths greater than 3 km (e.g. Liotta, 1996; Bonini and Sani, 2002; Acocella et al., 2002), leaving uncertainties in determining the geometry and location of the master fault in the area. The CROP03 deep seismic reflection profile shows an east-dipping reflector that from the eastern margin of the Siena-Radicofani Basin at the surface, reaches depths

of 4.0 s TWT, ~7 km. The same reflector displaces the top of the basement about 5 km to the east and has been interpreted as the east-dipping low-angle Radicofani Fault (RF) (Barchi et al., 1998; Decandia et al., 1998).

South of the CROP03 profile (Fig. 7a and b), the RF has been drilled by several boreholes where it emplaces the Ligurian units directly onto the Triassic evaporites, omitting the intervening Tuscan carbonate sequence completely (Fig. 7b). The eastern margin of the Radicofani Basin is controlled by the west-dipping high angle CF, which has been well documented at the surface (see below) and in seismic reflection profiles (Liotta, 1996; Acocella et al., 2002; Bonini and Sani, 2002), with an associated displacement of 1.5–2.0 km. We propose the east-dipping RF forms the master fault of the Radicofani area since: (a) the RF has a greater displacement than the CF; and (b) the RF has been detected down to 5 s TWT on the CROP03 deep seismic profile.

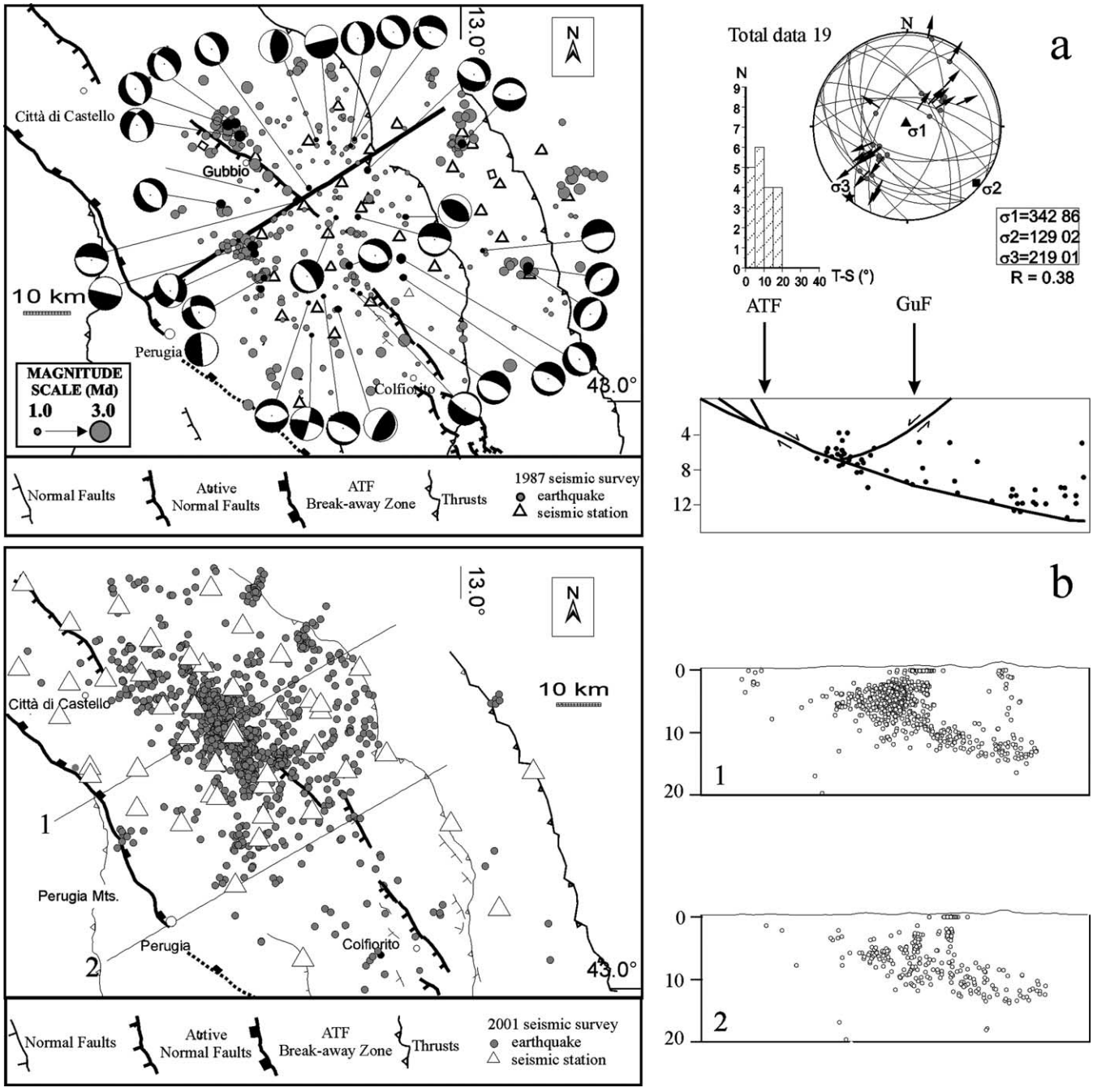

Fig. 6. Microseismic surveys. (a) May–June 1987 (Deschamps et al., 1989): map distribution, stress tensor analysis and cross-section. Focal mechanisms constrained by more than eight reliable P-wave first motion polarities. Hypocentral errors <2 km in the *XY* plane and <4 km in the *Z*-direction (Deschamps et al., 1989; Boncio et al., 2000). (b) October 2000–May 2001 (Piccinini et al., 2003). Mapped distributions and cross-sections of earthquakes with horizontal and vertical formal errors less than 1 km are shown in each case.

4.2. Geometry of the fault system at the surface

In order to investigate the surface expressions of extensional deformation, field structural data have been collected at eight localities (for locations, see Fig. 7) that occur both in the basin-fill sediments and the underlying substrate comprising the Ligurian and Tuscan sequences.

At the eastern margin of the Siena-Radicofani Basin, the west-dipping CF is well exposed at the surface (Fig. 8). The CF plane has an along-strike continuity of ~15 km, with a NNW–SSE trend and mean dip of ~70° with rare, approximately dip-slip, kinematic indicators (Fig. 8b). Associated fault breccias are up to ~15–20 m thick (Fig. 8c). At the surface, the CF marks the tectonic contact

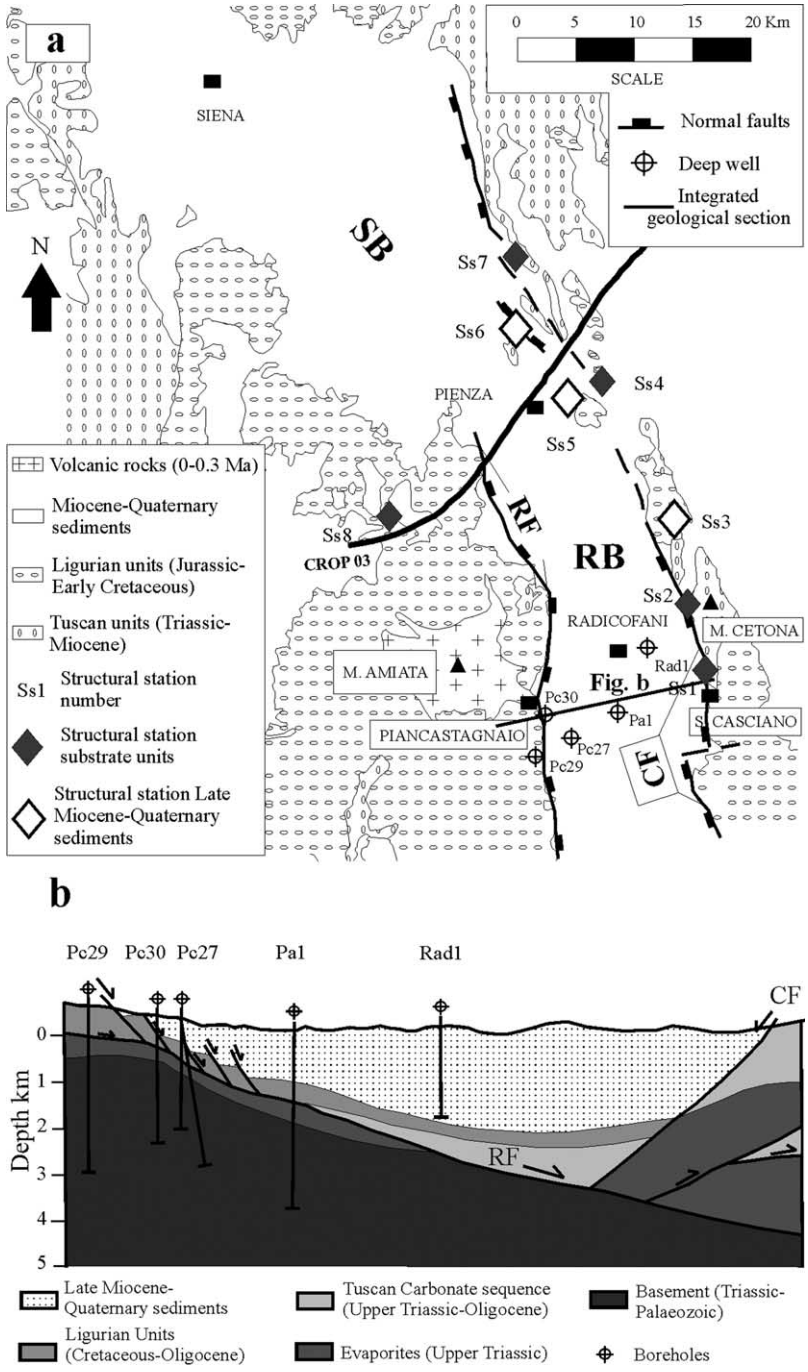

Fig. 7. (a) Schematic geological map of the Siena Basin, and Radicofani Basin (RB). (b) Interpretative geological section based on surface geology, seismic and borehole data (modified from Keller et al., 1994; Liotta, 1996). The east-dipping Radicofani normal fault, is interpreted as the main structure in the RB based on the CROP03 deep seismic reflection profile. The structural framework of the RB is completed by the steep antithetic, west-dipping, Cetona Fault and minor splays. Locations of boreholes also shown.

between the early-middle Pliocene, grey silty-clay rocks of the hanging wall block and the Triassic–Jurassic portion of the Tuscan carbonatic sequence in the footwall (Fig. 8a). Close to this contact, vertical synsedimentary tensile fractures filled with grey clay (early-middle Pliocene), have been observed parallel to the fault in the Liassic limestones located in the CF footwall (Fig. 8d). We interpret these features to indicate that normal faulting controlled clay-rich sediment deposition during Pliocene times.

The low-angle RF does not crop out (cf. Fig. 7b), but small-displacement normal faults and veins are preserved within the Pliocene sediments and the underlying substrate, which can be used to infer the age, geometry and kinematics of extension. The dominant structures in both the substrate and Pliocene sediments are NW–SE-trending conjugate normal faults exhibiting an Andersonian geometry (i.e. they are not rotated). Some NW–SE-trending faults within the Pliocene sediments show a typical thickening of the hanging wall beds (Fig. 9a), demonstrating growth faulting activity. Less numerous ∼E–W-trending faults are also present in the substrate units (Fig. 9, stereoplot 1). The small-scale normal faults display a more complicated pattern in the oldest units of the substrate compared with the youngest Pliocene sediments (Fig. 9, stereoplots 1–2). This pattern can be explained if the Triassic–Liassic sequences have experienced a longer, more complex deformation history since their deposition, whilst the structures within the Pliocene sediments record only the most recent phases of extension that formed the basin.

Vertical veins are widespread both in the Pliocene sediments and the Tuscan substrate (Fig. 9b, stereoplots 3–4). A more complex distribution, with two dominant families, trending, respectively, ∼NW–SE and ∼E–W, is present in the substrate. A simpler pattern occurs in the Pliocene sediments with ∼NW–SE-trending dominant sets. Some of these veins have been interpreted as synsedimentary structures, since the material filling the fractures is lithologically very similar to the Pliocene basin-filling sediments (Fig. 9b).

Small-displacement normal faults and veins do not show evidence of rotation. This implies that their orientation can be used to infer the related stress field that results in a vertical σ_1 and a SW–NE-trending σ_3 (Fig. 9, stereoplots 1–4). It is interesting to note that mesoscale extensional structures all display geometric and kinematic patterns consistent with the major structures recognized both in the

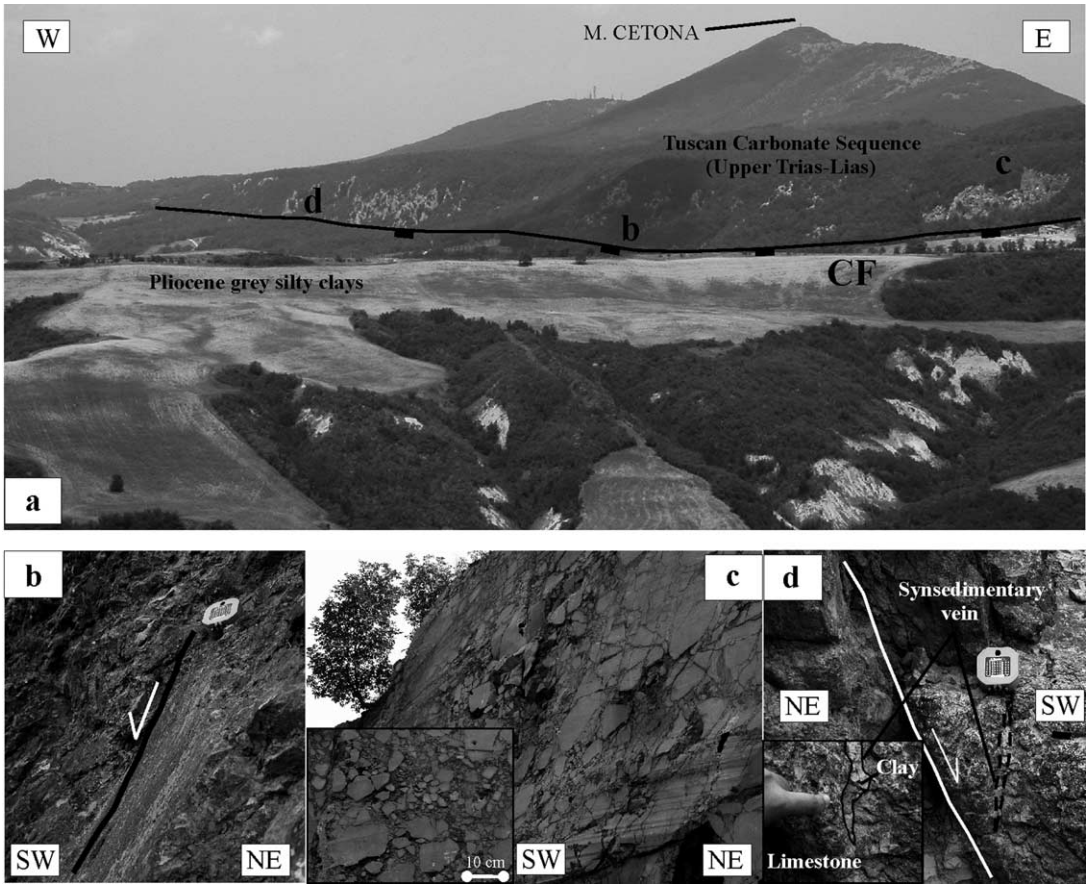

Fig. 8. (a) The Cetona Fault (CF), on the eastern margin of the RB (structural station Ss2 in Fig. 7) where hanging wall early-middle Pliocene grey silty clays are in tectonic contact with a footwall of Tuscan Carbonate Sequence rocks. The locations of Fig. 8b–d are also added). (b) The CF plane exposed at the surface. (c) Brecciated fault zone along the exposed CF. (d) Synsedimentary veins filled with middle Pliocene grey clays: these subvertical veins are located close to the CF (white line).

field and imaged using seismic profiles. In our interpretation, seismic reflection profiles and field data define a late Miocene–Pliocene extension accommodated by an east-dipping LANF and a contemporaneous antithetic high-angle normal fault. Extension is driven by a constant stress field with a vertical σ_1 and a SW–NE-trending σ_3.

5. The Zuccale fault system, Elba

The geological structure of the Isle of Elba (Fig. 10a and b) consists of five fault-bounded complexes stacked up during upper Cretaceous–lower Miocene Apenninic thrusting, which have been subsequently disrupted during a later phase of middle Miocene–lower Pliocene extension (Trevisan, 1950; Keller and Pialli, 1990). The final stages of extension were accompanied by the intrusion of granite porphyry sheets ca. 8 Ma (Rocchi et al., 2002), the M. Capanne granodiorite ca. 7 Ma (Saupé et al., 1982) and the Porto Azzurro monzogranite with associated dykes ca. 5.1 Ma (Saupé et al., 1982).

Two major, east-dipping low-angle normal faults with kilometre-scale displacements are considered to be particularly significant extensional structures in the area (Fig. 10a): the Capanne fault, formed synchronously with the intrusion of the Monte Capanne pluton (Daniel and Jolivet, 1995) and the Zuccale Fault (ZF) (Trevisan, 1950; Keller and Pialli, 1990; Keller and Coward, 1996; Bortolotti et al., 2001; Collettini and Holdsworth, 2004); the latter structure is particularly well exposed in parts of the island (Figs. 11 and 12).

5.1. Architecture and kinematics

The thrust sheet complexes, locally intruded by 8 Ma porphyry sheets in central and eastern Elba, are disrupted and offset by the ZF cutting down-section and displacing its hanging wall towards the east (Fig. 10b; Trevisan, 1950). The ZF shows predominant eastward dips, in the range 10–20°, although some locally west-dipping segments occur associated with variably back-rotated arrays of small displacement listric normal faults located in the footwall (see below). Field

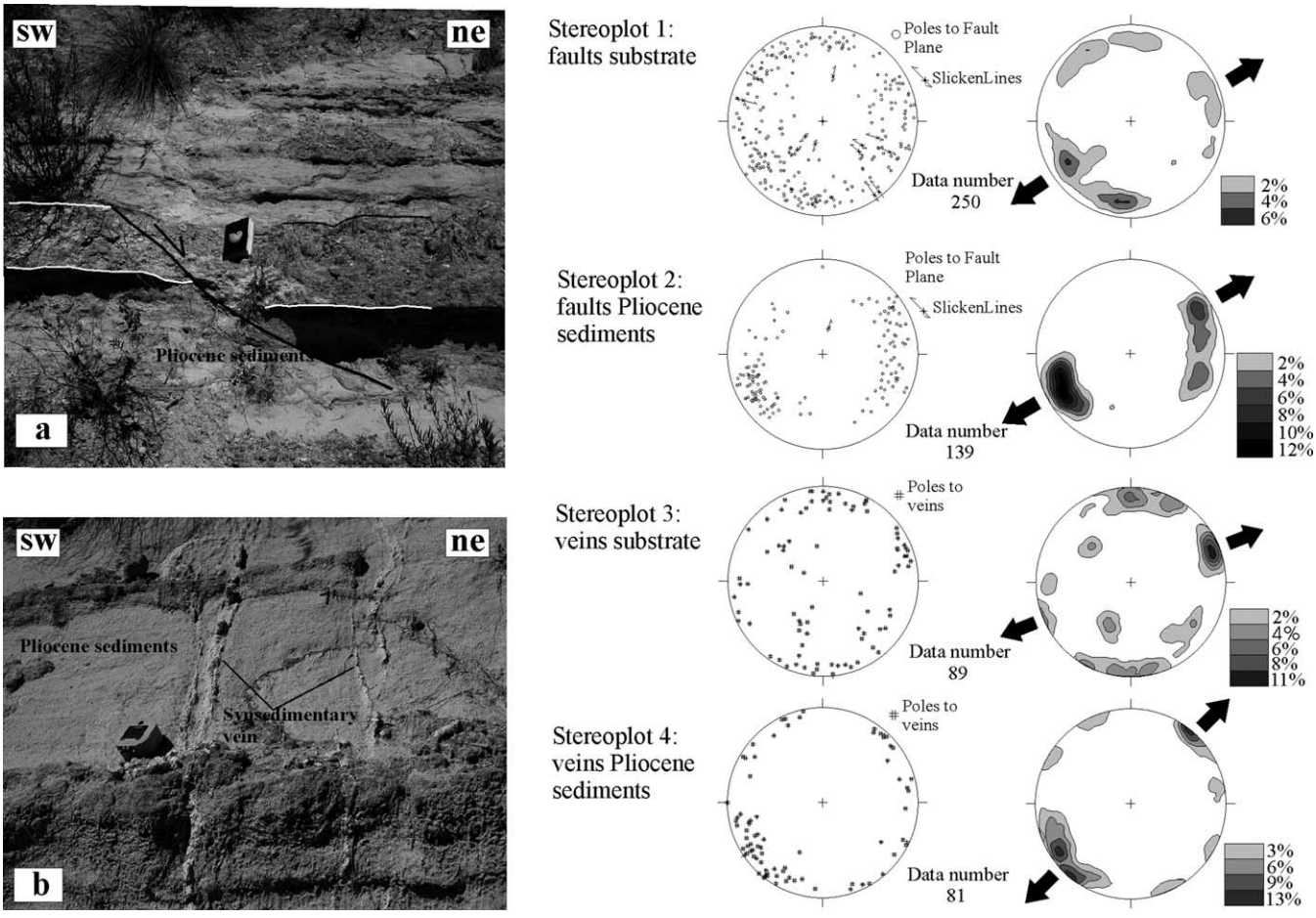

Fig. 9. Extension within the Radicofani basin: (a) synsedimentary fault indicated by hanging-wall bed thickening (structural station Ss5; for location see Fig. 7a). (b) Synsedimentary veins filled with fine grained sediments in the Pliocene sediments (structural station Ss5). Stereoplots 1–2 (equal area projection, lower hemisphere) display all the normal faults observed in the substrate units and Pliocene sediments, respectively. Regional orientation of extension, NE–SW oriented (black arrows). Stereoplots 3–4 (equal area projection lower hemisphere) display the synsedimentary veins in the substrate units and Pliocene sediments, respectively.

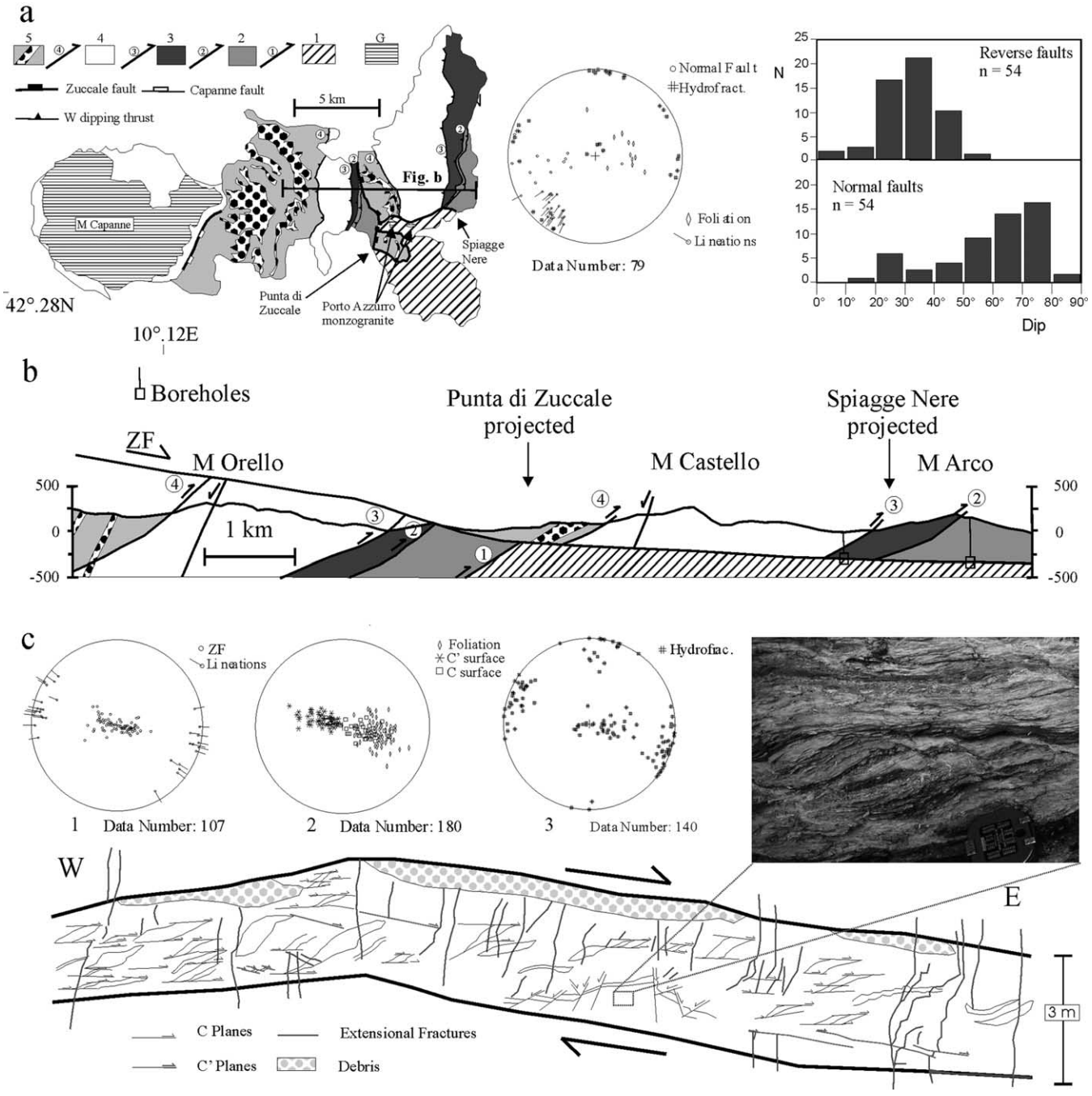

Fig. 10. (a) Schematic geological and structural map of the Isle of Elba: G, Mt. Capanne granodiorite ca. 7 Ma and Porto Azzurro monzogranite 5.1 Ma; 1, Complex I, basement schists; 2, Complex II, Tuscan metamorphic sequence; 3, Complex III, Tuscan carbonate sequence; 4, Complex IV, Ligurian ophiolites; 5, Complex V, late Cretaceous flysch intruded by granite porphyry ca. 8 Ma. Stereoplot (equal area projection, lower hemisphere) showing poles to basement foliations and associated lineations, poles to hydrofractures and poles to normal faults in the footwall of the Zuccale Fault (ZF). Normal and reverse fault dip-distribution: data have been collected within the 4 complexes in the hanging wall of the ZF and show Andersonian dips (modified after Collettini and Holdsworth, 2004). (b) Geological cross-section through central and eastern Elba. The section has been constructed along section 1 of the geological map of Elba (Trevisan et al., 1967). The ZF position at depth has been located using borehole data (Bortolotti et al., 2001). (c) Cartoon showing the ZF zone architecture at Punta di Zuccale. Structures within the fault zone are consistent with a top-to-the-east sense of shear; stereoplots are equal area projection, lower hemisphere with structural surfaces plotted as poles (modified after Collettini and Barchi, 2004). In the photograph details of the C-type and C′-type shear bands within the fault zone are shown.

data collected within the four complexes exposed in the hanging wall of the ZF reveal the presence of small displacement normal and reverse-slip faults with classical Andersonian dips (histograms in Fig. 10a), suggesting that no substantial passive rotation of the hanging wall block has occurred. In the basement schists of the footwall block, SW-dipping foliation and NNE–SSW-trending lineations are preserved and are thought to be related to earlier pre-

Mesozoic ductile deformation. These are everywhere cross-cut by brittle normal faults and joints developed during the extensional phase (Fig. 10a, stereoplot). The ZF is a regional feature and its offshore continuation is recognised both on the mainland at depth along the CROP03 seismic profile (Barchi et al., 1998; Fig. 1b) and in a seismic profile crossing the along-strike, southern projection of the fault, 20 km south of Elba (Keller and Coward, 1996). Here, the ZF is associated with steeply dipping antithetic structures, with displacement estimates ranging from at least 7 to 9 km based on stratigraphic offsets (Keller and Coward, 1996). The ZF is the most important fault of the island acting from 13 to 4 Ma and the exposed fault rocks are exhumed from depths in the range 3–6 km (Collettini and Holdsworth, 2004).

The fault zone architecture and kinematics have been studied at two different localities where the fault is well exposed, Punta di Zuccale and Spiagge Nere (for locations see Fig. 10a). At Punta di Zuccale, the ZF separates a hanging wall sequence of upper Cretaceous, argillacious–calcareous, Helminthoid flysch (Complex V) from a footwall of Palaeozoic, muscovite–biotite, basement schists and localised Triassic sediments of the Verrucano formation (Complex I). The fault zone (Fig. 10c) is characterised by strongly foliated, 'ductile' fault rocks (sensu Rutter, 1986) derived from cataclasites, carbonate mylonites and ultramafic units with interdispersed, fluid-induced hydrofracture veins filled with carbonate (Collettini and Barchi, 2004; Collettini and Holdsworth, 2004). The surface of the ZF is undulatory with prevailing eastward dips and subordinate west-dipping surfaces (Fig. 11c, stereoplot 1). The mean trend of the fault is ~N–S and the distribution of the slickenlines striae and aligned calcite fibres gives a N110°E direction of movement (Fig. 10c, stereoplot 1). The fault zone is characterised by abundant C-type and C′-type shear bands (sensu Berthé et al., 1979), bounding S-foliated domains homogeneously distributed within the fault zone (details in Fig. 10c, stereoplot 2). All these structures indicate top-to-the-east senses of shear. The fault zone is also affected by abundant carbonate-filled hydrofractures (Fig. 10c, stereoplot 3) showing crack-seal textures and geometries consistent with syntectonic tensile fracturing in a stress field with vertical σ_1 (Collettini and Barchi, 2004).

At Spiagge Nere, the ZF separates a hanging wall sequence of various rock types belonging to Complexes II and III, from a footwall of Palaeozoic, muscovite–biotite-rich basement schists (Complex I). The ZF attitude at this locality is undulatory, with either west or east shallow-dipping segments (Fig. 11, stereoplot 1). The orientation of the slickenlines is consistent with an E–W-trending direction of movement (Fig. 11, stereoplot 1), with all shear sense indicators giving top-to-the-east sense of movement. The fault zone once again comprises strongly foliated cataclasites derived from various protolith lithologies (carbonates and ultramafics), and is similar to the Punta di Zuccale exposure. The kinematic indicators within the fault zone are mostly east-dipping C-type and subhorizontal C′-type shear bands, bounding prevailing west-dipping S surfaces (Fig. 11, stereoplot 2). The majority of syn-kinematic, high-angle normal faults in the hanging wall block sole into the detachment surface (e.g. Fig. 11).

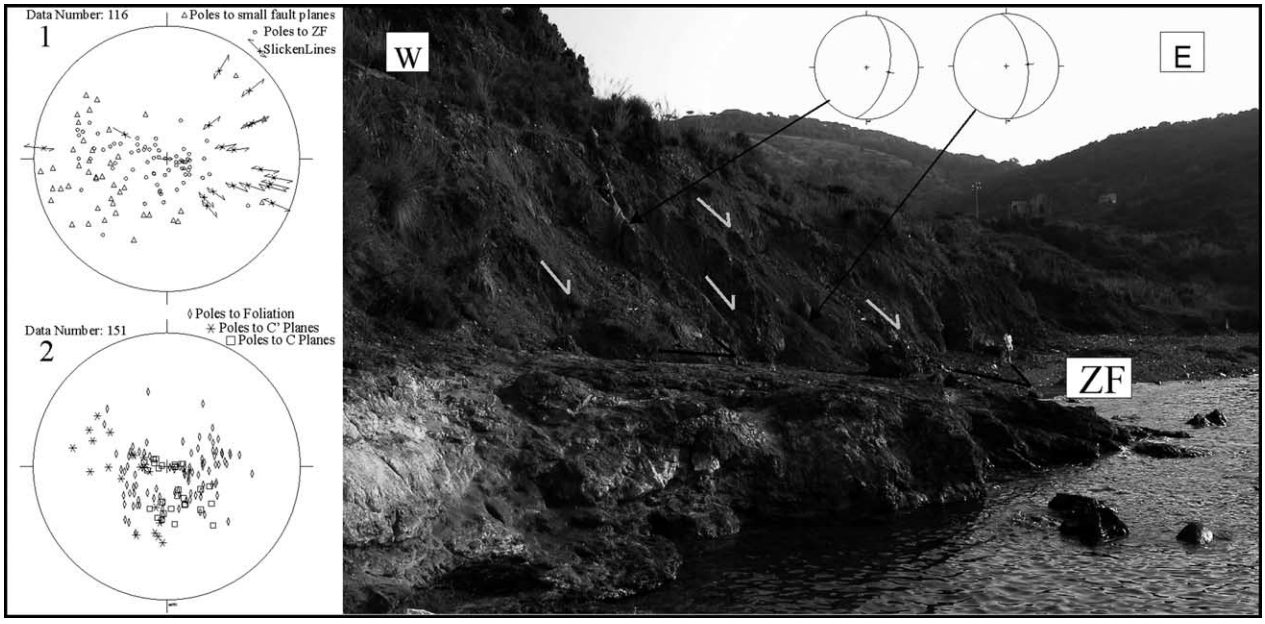

Fig. 11. The Zuccale Fault (ZF) and associated structures at Spiagge Nere (for location see Fig. 10). Moderately- to steeply-dipping 'Andersonian' normal faults in the hanging wall of the ZF sole into the main low-angle detachment. The two stereoplots within the figure show the two normal fault planes and associated down-dip slickenlines. Stereoplots to the left summarise the key structures within the fault zone (equal area projection, lower hemisphere): the ZF plane gently dips toward east and is associated with minor east-dipping high angle normal faults, the slickenlines are shallowly plunging toward the east (stereoplot 1); the foliated fault core is affected by C-type and C′-type shear bands bounding S-foliated domains consistently with top-to-the-east sense of shear.

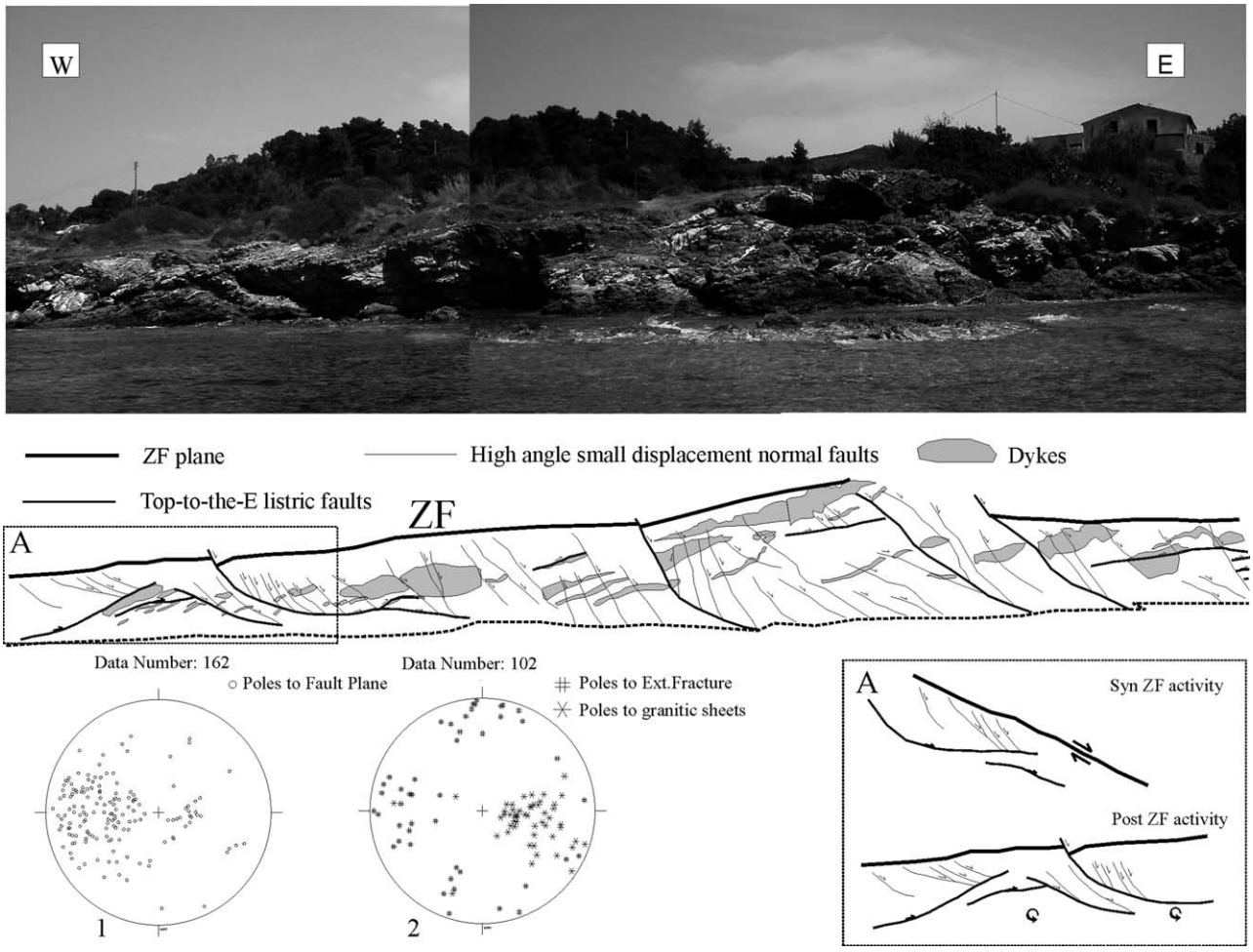

Fig. 12. Footwall architecture of the Zuccale Fault (ZF) at Spiagge Nere (for location see Fig. 10) where listric normal faults and synthetic high angle structures result in very minor passive reorientation of the ZF (stereoplot 1, equal area projection, lower hemisphere). This faulting episode is of limited importance at a regional scale and generally cross-cuts the granite sheets (see text for details). The N–S-trending granitic sheets display a wide range of dips between 5 and 85°, the calcite filled hydrofractures are organized in two orthogonal families, respectively, E–W and N–S-trending (stereoplot 2, equal area projection, lower hemisphere). The inset shows a partial block rotation reconstruction for the fault system enclosed in box A.

The deformation in the ZF footwall block is spectacularly exposed at Spiagge Nere (Fig. 12), where both east- and west-dipping, top-to-the-east, curviplanar listric faults are well exposed, generally carrying a well-developed zone of foliated cataclasite (heavy grey lines on Fig. 12). Numerous high-angle small-displacement normal faults are located in the hanging walls of the listric structures; a smaller number of high-angle faults show apparently reverse displacements. N–S-trending, west-dipping granitic sheets associated with the Porto Azzurro monzogranite, are also widely developed and possess a wide range of dips between 5 and 85° (Fig. 12, stereoplot 2). These structures formed together with more minor N–S- and E–W-trending vertical hydrofractures filled with quartz and tourmaline (Fig. 12, stereoplot 2). Whilst all normal faults cross-cut the granite sheets, only the earliest-formed, west-dipping listric faults preserve granite sheets smeared out within fault zones suggesting emplacement synchronous with faulting. We interpret this complex normal fault system to result from a series of localised block rotations in the footwall of the ZF (e.g. Fig. 12, inset). The presently west-dipping reverse faults are thought to represent originally east-dipping normal faults reoriented by block rotations associated with the east-dipping listric structures. The block rotation model thus explains: (1) the presently west-dipping attitude of some portions of the ZF; (2) the apparent reverse offsets of sheets along some faults located at the hanging wall of larger, listric east-dipping structures; and (3) the observed wide dip-range of the granitic sheets. It is important to note that the fault systems preserved in the ZF footwall have only a limited importance on a regional scale and we suggest that only minor passive reorientation of the ZF has occurred.

Field data collected in the Isle of Elba demonstrate clearly that the east-dipping, low-angle ZF is the most important structure in accommodating extension. Extensional movements occurred on the fault at low-angle dips and in a state of stress characterised by vertical σ_1 as confirmed by the preservation of: (i) high-angle normal

faults that sole into the ZF (Fig. 11); (ii) classical Andersonian thrusts and normal faults in the hanging wall block (Fig. 10, histograms); and (iii) the dominantly vertical orientation of syn-kinematic hydrofractures throughout (Fig. 10c).

6. The Northern Apennines extensional system: architecture, geometry and mechanics

6.1. Geometry and kinematics of the extensional systems

Along the studied crustal transect, the three investigated areas show similar structural features in which upper crustal extension is accommodated by east-dipping low-angle normal faults and associated steeper-dipping east- and west-dipping synthetic and antithetic structures, respectively. In this linked fault system, the LANFs are the master faults, individually accommodating several kilometres of displacement (typically in the order of 5–10 km). They possess well-developed fault zones preserved both in outcrop (up to 20 m thick) and also as continuous reflectors well-imaged in seismic profiles. In the LANF hanging wall regions, important high-angle normal faults possessing an along strike continuity of ~20 km accommodate displacements in the order of 1–3 km. This geometry has been documented both in the Umbria region associated with the east-dipping Altotiberina fault and the antithetic high angle Gubbio normal fault, and in Tuscany with the east-dipping Radicofani fault and the high angle west-dipping Cetona fault. In Elba, west-dipping normal faults represent minor structures, although offshore seismic reflection profiles located to the south of the island show that the east-dipping low-angle Zuccale fault is associated with west-dipping antithetic structures (Keller and Coward, 1996).

Field-based structural orientation data and kinematic observations together with earthquake focal mechanisms can be used to infer the orientation of extension at different times along our Apennine transect. In all areas, extensional movements occur in a stress field characterised by a regional vertical σ_1 and NE–SW (Tuscan mainland and Umbria)- to E–W (Elba)-trending subhorizontal σ_3.

During the final stage of extension, the geometry of the LANF becomes locally subhorizontal or gently west-dipping. The dip variations probably result from gentle back-rotation, possibly during regional footwall unloading (e.g. Wernicke and Axen, 1988), uplift and pluton emplacement, as illustrated on the Isle of Elba. Though the west-dipping antithetic structures in the Northern Apennines show a smaller displacement (1–3 km), they severely influence the topography and possibly for this reason have been considered previously to be the main extensional structures in the Umbria–Marche Apennines (e.g. Lavecchia et al., 1994). In the extending zone of the Umbria–Marche Apennines, it is these faults that are responsible for the strongest earthquakes.

6.2. Fluid involvement in extensional processes

The extended/extending sector of the Northern Apennines is characterised by an anomalous crustal flux of deep-sourced CO_2, probably related to mantle degassing. The mapped anomaly is widespread in Tuscany and, moving eastwards, seems to vanish immediately east of the active extensional front in the Umbria–Marche Apennines (Chiodini et al., 2004). During their ascent through the crust, fluids can become trapped by stratigraphic or structural seals favouring the attainment of fluid overpressures. The deeply sourced CO_2 degassing potentially represents a renewable fluid-supply continuously rising into the brittle crust during the entire fault history. A fossil example of this process may be represented by the complex syntectonic vein systems associated with the ZF where the crack-seal textures of the hydrofractures testify to cyclic build ups in fluid overpressure during fault activity (Collettini and Barchi, 2004; Collettini and Holdsworth, 2004). Fluid overpressures are well documented in the Umbria–Marche Apennines, where two boreholes, San Donato and Pieve Santo Stefano, recorded fluid overpressures of ~100 and 70 MPa at depths of ~5000 and 4000 m, respectively, corresponding to a pore fluid pressure close to 80% of the lithostatic load (Fig. 13). Fluid overpressure may also play an important role in triggering microseismicity on the low-angle Altotiberina fault (Collettini and Barchi, 2002), or for explaining a protracted seismic sequence involving the nucleation of a series of mainshocks in a short time interval during the 1997 Colfiorito sequence (Miller et al., 2004).

6.3. The mechanics of LANFs

Any model to explain the presence of LANFs in the Northern Apennines needs to account for both the initiation of such faults and their continued activity over long time periods that allow them to accommodate the observed kilometre-scale displacements.

LANF initiation: Doglioni et al. (1999) have proposed a kinematic model to explain the eastward-migrating pulse of extension observed following compression in which subduction roll-back occurs below the Apenninic mountain chain. According to Doglioni and co-workers, the eastward retreat of the W-dipping subduction zone would likely lead to eastward-migrating mantle flow which would generate a significant shear stress at the base of the overlying brittle crust, with this effect decreasing to the west (Fig. 13; Doglioni et al., 1999). This ‘differential drag’ affecting the deeper parts of the crust overlying the retreating slab would favour transient stress tensor rotation in the region immediately above the subducting plate, close to the transition between active compression and extension in the crust (cf. Westaway, 1999; Doglioni et al., 1999). Rotations of up to 45° could occur, resulting in an east-dipping σ_1 which would promote the initiation of shallowly east-dipping LANFs. During this initial phase, fault-growth

within the brittle upper crust would be achieved by the linking together of pre-existing east-dipping discontinuities, i.e. back-thrusts and/or tilted bedding formed during the compressional phase, possibly promoted by the transient development of high pore fluid pressures.

Longer-term movement and continued accumulation of slip along LANFs: according to the model presented here, continued movement would have to occur along low-angle structures in the brittle upper crust where σ_1 possesses a sub-vertical orientation: this requires long-term weakening of the fault zones.

The coincidence in timing of plutonism (5–8 Ma) and extension along the ZF (13–4 Ma) superficially suggests that thermal weakening related to the intrusion of magmas could play a part in facilitating low-angle fault movement (cf. the Capanne fault, Daniel and Jolivet, 1995). Collettini and Holdsworth (2004) suggest that this is unlikely for the ZF because the detachment was clearly active as a low-angle normal fault in offshore locations far from granitic plutons (e.g. Keller and Coward, 1996). In addition, the ZF cross-cuts everywhere the granitic intrusions in both the footwall and hanging wall and all fault-related deformation in the footwall appears to be brittle. Finally, there is no evidence to suggest that the currently active Altotiberina low-angle normal fault is associated with magmatic activity.

The exhumed fault rocks from the ZF in the Isle of Elba provide abundant and compelling evidence of the nature of such weakening mechanisms in the brittle crust below 3 km (Collettini and Holdsworth, 2004). Field-based and micro-structural studies suggest an evolution from an initial brittle cataclasite to a narrow foliated fault core formed as the result of syntectonic fluid–rock interactions. Fluids reacted with the fine-grained cataclasite to produce fine-grained aggregates of weak phyllosilicate-rich fault rocks leading to reaction softening. In addition, the fine grain sizes trigger the widespread onset of stress-induced dissolution and precipitation processes. The resulting fault rock textures are very similar to those formed during pressure-solution-accommodated 'frictional-viscous' creep in experimental phyllosilicate-rich fault rock analogues (Bos and Spiers, 2001, 2002). Microphysical models based on these analogue experiments predict a switch from a cataclastic deformation to a pressure solution-accommodated frictional slip resulting in a highly organised foliated microstructure with abundant C- and C′-type shear bands very similar to those preserved along the ZF (cf. Fig. 11 in Collettini and Holdsworth, 2004). In the experimental analogues, the switch in rheology is associated with a decrease in friction from Byerlee's values to ~0.2 or less. With a friction coefficient of 0.2, LANFs such as those observed in the Northern Apennines could move easily in a stress field with vertical σ_1. Furthermore, such weak faults would be incapable of generating big earthquakes because at low-sliding velocity the pressure-solution accommodated deformation is a velocity strengthening process favouring aseismic slip (Collettini and Holdsworth, 2004). The microseismic activity recorded along the Altotiberina fault would be promoted by local short-lived cyclic build-ups in fluid overpressure, as recorded in the San Donato borehole, leading to hydrofracturing and veining as observed along the exhumed ZF.

7. Conclusions

The Northern Apennines of Italy are in some ways as important as the Basin & Range region of the USA as they

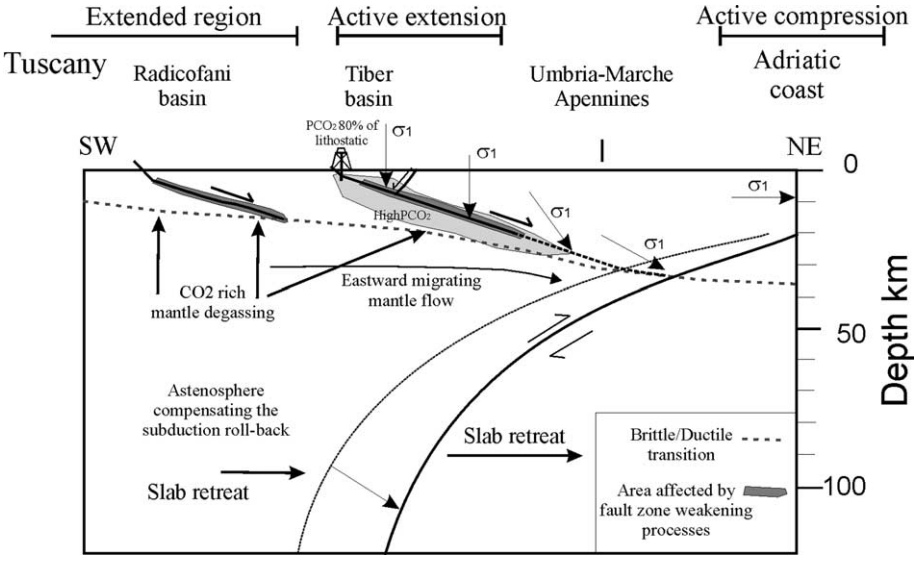

Fig. 13. Model for the initiation and (re)activation of low-angle normal faults based on the kinematic model proposed by Doglioni et al. (1999) for the migration of the extension–compression pair in the hanging wall of the Apenninic west-directed subduction zone. Arrows labelled σ_1 show proposed orientation of the maximum principal stress moving westwards, away from retreating slab. The upper crust stress tensor is constrained by surface geology, borehole breakouts and earthquake focal mechanisms. The location of the brittle–ductile transition after Pauselli and Federico (2002).

represent a natural laboratory in which the key role played by LANFs in accommodating crustal extension may be examined. Regional extension has been a continuous process, migrating progressively from west to east, with east-dipping LANFs acting as regional detachments, accommodating a majority of the extension in the Northern Apennines. Differential exhumation of the crust means that originally deeper sections of the normal fault zones are now exposed at the surface in the older parts of the system, giving direct insights into processes down to the uppermost middle crust during extension. Regionally, the stress field was characterised by a vertical σ_1 and a NE–SW (Tuscan mainland and Umbria)- to E–W (Elba)-trending σ_3. For LANFs to be active in such a stress field, the fault zones have to be anomalously weak over long time-scales (millions of years). Good evidence for such weakening is exposed at the surface where the deeper parts of the LANF detachments possess a well-developed fault core of foliated fault rocks in which fluids have triggered reaction softening and the onset of stress-induced solution-precipitation mechanisms in cataclastic rocks formed at depths of as little as 3 km. Comparison with the results of recent deformation experiments of analogue materials suggests that such processes will lead to frictional-viscous slip behaviour at much reduced friction coefficients ($\mu_s < 0.2$). Our findings suggest, therefore, that LANFs are able to move as low-angle structures and to accommodate large displacements. The weakness of the faults also explains the observed lack of large magnitude earthquakes along such structures (Collettini and Holdsworth, 2004). Once established, the foliated fault cores also act as effective seals leading to cyclic overpressuring, triggering microseismicity which is now widely recognised along the LANF of the Northern Apennines.

We speculate that the initiation of E-dipping normal faults with relative low-angles of dip may reflect differential drag generated by mantle flow following slab retreat and roll-back beneath the Apennine chain. Thus large-scale asymmetric crustal extension facilitated by LANFs may be particularly common in regions where subduction roll-back occurs, especially if there is an associated mantle-derived fluid flux to promote long-term weakening of the crustal faults following their initiation.

Acknowledgements

We thank R. Di Stefano for providing seismological data in Fig. 2 and L. Chiaraluce for fruitful discussions. We thank C. Doglioni and S. Marshak for constructive reviews.

References

Acocella, V., Pascucci, V., Dominici, G., 2002. Basin deformation due to laccolith emplacement at Radicofani Southern Tuscany, Italy. Boll. Soc. Geol. It., Vol. Spec. 1, 749–756.

Ambrosetti, P., Carboni, M.G., Conti, M.A., Costantini, A., Esu, D., Gadin, A., Girotti, O., Lazzarotto, A., Mazzanti, R., Nicosia, U., Parisi, G., Sandrelli, F., 1978. Evoluzione paleogeografica e tettonica dei bacini tosco-umbro-laziali nel Pliocene e nel Pleistocene inferiore. Mem. Soc. Geol. It. 19, 573–580.

Anelli, L., Gorza, M., Pieri, M., Riva, M., 1994. Subsurface well data in the Northern Apennines. Mem. Soc. Geol. It. 48, 461–471.

Axen, G.J., 1992. Pore pressure, stress increase, and fault weakening in low-angle normal faulting. J. Geophys. Res. 97, 8979–8991.

Axen, G.J., 1999. Low-angle normal fault earthquakes and triggering. Geophys. Res. Lett. 26, 3693–3696.

Barchi, M.R., Minelli, G., Pialli, G., 1998. The crop 03 profile: a synthesis of results on deep structures of the Northern Apennines. Mem. Soc. Geol. It. 52, 383–400.

Barchi, M.R., Paolacci, S., Pauselli, C., Pialli, G., Merlini, S., 1999. Geometria delle deformazioni estensionali recenti nel bacino dell'Alta Val Tiberina fra S. Giustino Umbro e Perugia: evidenze geofisiche e consideraioni geologiche. Boll. Soc. Geol. It. 118, 617–625.

Barchi, M.R., Galadini, F., Lavecchia, G., Messina, P., Michetti, A.M., Peruzza, L., Pizzi, A., Tondi, E., Vittori, E., 2000. Sintesi sulle conoscenze delle faglie attive in Italia Centrale. Gruppo Nazionale per la Difesa dei Terremoti, 62pp.

Berthé, D., Choukroune, P., Jegouzo, P., 1979. Orthogneiss, mylonite and non-coaxial deformation of granites: the example of South Armorican Shear Zone. J. Struct. Geol. 1, 31–42.

Boncio, P., Brozzetti, F., Lavecchia, G., 1996. State of stress in the Northern Umbria-Marche Apennines (Central Italy): inferences from microearthquakes and fault kinematics analyses. Annales Tectonicae 10, 80–97.

Boncio, P., Brozzetti, F., Lavecchia, G., 2000. Architecture and seismotectonics of a regional low-angle normal fault zone in central Italy. Tectonics 19, 1038–1055.

Bonini, M., Sani, F., 2002. Extension and compression in the Northern Apennines (Italy) hinterland: evidence from the late Miocene–Pliocene Siena-Radicofani basin and relations with basement structures. Tectonics 213. doi:10.1029/2001TC900024.

Borraccini, F., De Donatis, M., Di Bucci, D., Mazzoli, S., Megna, A., Nesci, O., Santini, S., Savelli, D., Tramontana, M., Triggiani, P., 2002. Analisi della tettonica quaternaria nel basso bacino del fiume Metauro Marche settentrionali e nell'adiacente offshore adriatico attraverso l'integrazione di dati sismici, geomorfologici, stratigrafici e strutturali. Studi Geologici Camerti 2, 29–44.

Bortolotti, V., Fazzuoli, M., Pandeli, E., Principi, G., Babbini, A., Corti, S., 2001. Geology of central and eastern Elba Island, Italy. Ofioliti 26, 97–150.

Bos, B., Spiers, C.J., 2001. Experimental investigation into the microstructural and mechanical evolution of phyllosilicate-bearing fault rock under conditions favouring pressure solution. J. Struct. Geol. 23, 1187–1202.

Bos, B., Spiers, C.J., 2002. Frictional-viscous flow of phyllosilicate-bearing fault rock: microphysical model and implications for crustal strength profiles. J. Geophys. Res. 107 (B). doi:10.1029/2001JB000301.

Boschi, E., Guidoboni, E., Ferrari, G., Valensise, G., 1998. I terremoti dell'Appennino Umbro-Marchigiano area sud orientale dal 99 a.C. al 1984—ING-SGA.

Brozzetti, F., 1995. Stile deformativo della tettonica distensiva nell'Umbria Occidentale: l'esempio dei Massicci Mesozoici Perugini. Studi Geologici Camerti 1, 105–119.

Carmignani, L., Decandia, F.A., Fantozzi, P.L., Lazzarotto, A., Liotta, D., Meccheri, M., 1994. Tertiary extensional tectonics in Tuscany Northern Apennines, Italy. Tectonophysics 238, 295–315.

Chiaraluce, L., Ellsworth, W.L., Chiarabba, C., Cocco, M., 2003a. Imaging the complexity of an active normal fault system: the 1997 Colfiorito (Central Italy) case study. J. Geophys. Res. 108 (B6), 2294. doi:10.1029/2002JB002166.

Chiaraluce, L., Piccinini, D., Chiarabba, C., 2003b. High resolution micro-seismicity data constraining the geometry and kinematics of an

active very low-angle normal fault in the Northern Apennines (Central Italy). Geophys. Res. Abs. 5, 11930. EGS.

Chiodini, G., Cardellini, C., Amato, A., Boschi, E., Caliro, S., Frondini, F., Ventura, G., 2004. Carbon dioxide Earth degassing and seimogenesis in central and southern Italy. Geophys. Res. Lett. 31, L07615. doi:10.1029/2004GL019480.

Collettini, C., Barchi, M.R., 2002. A low angle normal fault in the Umbria region (Central Italy): a mechanical model for the related microseismicity. Tectonophysics 359, 97–115.

Collettini, C., Barchi, M.R., 2004. A comparison of structural data and seismic images for low-angle normal faults in the Northern Apennines (Central Italy): constraints on activity. In: Alsop, G.I., Holdworth, R.E. (Eds.), Flow Processes in Faults and Shear Zones Journal of the Geological Society, London, Special Publications 224, pp. 95–112.

Collettini, C., Holdsworth, R.E., 2004. Fault zone weakening processes along low-angle normal faults: insights from the Zuccale Fault, Isle of Elba, Italy. J. Geol. Soc. 161, 1039–1051.

Collettini, C., Sibson, R.H., 2001. Normal faults normal friction? Geology 29, 927–930.

Collettini, C., Barchi, M.R., Chiaraluce, L., Mirabella, F., Pucci, S., 2003. The Gubbio fault: can different methods give pictures of the same object? J. Geodyn. 36/1-2, 51–66.

Daniel, J.M., Jolivet, L., 1995. Detachments faults and pluton emplacement: Elba island Tyrrhenian Sea. Bull. Soc. Géol. Fr. 166, 341–354.

De Franco, R., Ponziani, F., Biella, G., Boniolo, G., Caielli, G., Corsi, A., Maistrello, M., Morrone, A., 1998. DSS-WAR experiment in support of the CROP03 project. Mem. Soc. Geol. It. 52, 67–90.

Decandia, F.A., Lazzarotto, A., Liotta, D., Cernobori, L., Nicolich, R., 1998. The CROP 03 traverse: insights on post-collisional evolution of the Northern Apennines. Mem. Soc. Geol. It. 52, 413–425.

Deschamps, A., Iannaccone, D., Scarpa, R., 1984. The Umbrian earthquake (Italy) of 19 September 1979. Ann. Geophys. 2, 29–36.

Deschamps, A., Scarpa, R., Selvaggi, G., 1989. Analisi sismologica del settore settentrionale dell'Appennino umbro-marchigiano. Atti GNGTS 8th Conference 1, pp. 9–15.

Di Stefano, R., Chiarabba, C., Lucente, F., Amato, A., 1999. Crustal and uppermost mantle structure in Italy from inversion of P-wave arrival times: geodynamic implications. Geophys. J. Int. 139, 483–498.

Doglioni, C., Harabaglia, P., Merlini, S., Mongelli, F., Peccerillo, A., Piromallo, C., 1999. Orogens and slabs vs. their direction of subduction. Earth Sci. Rev. 45, 167–208.

Dziewonski, A.M., Franzen, J.E., Woodhouse, J.H., 1985. Centroid-moment tensor solutions for April–June, 1984. Phys. Earth Planet. In. 37, 87–96.

Ekström, G., Morelli, A., Boschi, E., Dziewonski, A.M., 1998. Moment tensor analysis of the central Italy earthquake sequence of September–October 1997. Geophys. Res. Lett. 25, 1971–1974.

Elter, P., Giglia, G., Tongiorgi, M., Trevisan, L., 1975. Tensional and contractional areas in recent Tortonian to Present evolution of the Northern Apennines. Bollettino di Geofisica Teorica ed Applicata 17, 1975.

Finetti, I., Boccaletti, M., Bonini, M., Del Ben, A., Geletti, R., Pipan, M., Sani, F., 2001. Crustal section based on CROP seismic data across the north Tyrrhenian–Northern Apennines Adriatic Sea. Tectonophysics 343, 135–163.

Frepoli, F., Amato, A., 1997. Contemporaneous extension and compression in the Northern Apennines from earthquake fault-plane solutions. Geophys. J. Int. 139, 483–498.

Gasparini, C., Iannaccone, G., Scarpa, R., 1985. Fault-plane solutions and seismicity of the Italian peninsula. Tectonophysics 117, 59–78.

Haessler, H., Gaulon, R., Rivera, L., Console, R., Frogneux, M., Gaparini, G., Martel, L., Patau, G., Siciliano, M., Cisternas, A., 1988. The Perugia (Italy) earthquake of 29, April 1984; a microearthquake survey. Bull. Seismol. Soc. Am. 78, 1948–1964.

Hunstad, I., Selvaggi, G., D'Agostino, N., England, P., Clarke, P., Pierozzi, M., 2003. Geodetic strain in peninsular Italy between 1875 and 2001. Geophys. Res. Lett. 30 (4), 1181. doi:10.1029/2002GL016447.

Jackson, J.A., White, N.J., 1989. Normal faulting in the upper continental crust: observation from regions of active extension. J. Struct. Geol. 11, 15–36.

Jolivet, L., Faccenna, C., Goffé, B., Mattei, M., Rossetti, F., Brunet, C., Storti, F., Funiciello, R., Cadet, J.P., D'Agostino, N., Parra, T., 1998. Midcrustal shear zones in postorogenic extension: example from the northern Tyrrhenian Sea. J. Geophys. Res. 103B6, 12123–12160.

Keller, J.V.A., Coward, M.P., 1996. The structure and evolution of the Northern Tyrrhenian Sea. Geol. Mag. 133, 1–16.

Keller, J.V.A., Pialli, G., 1990. Tectonics of the island of Elba: a reappraisal. Boll. Soc. Geol. It. 109, 413–425.

Keller, J.V.A., Minelli, G., Pialli, G., 1994. Anatomy of late orogenic extension: the Northern Apennines case. Tectonophysics 238, 275–294.

Lavecchia, G., Stoppa, F., 1990. The Tyrrhenian zone: a case of lithosphere extensional tectonic control of intra-continental magmatism. Earth Planet. Sc. Lett. 99, 336–350.

Lavecchia, G., Brozzetti, F., Barchi, M.R., Keller, J.V.A., Menichetti, M., 1994. Seismotectonic zoning in east-central Italy deduced from the analysis of the Neogene to present deformations and related stress fields. Geol. Soc. Am. Bull. 106, 1107–1120.

Lavecchia, G., Boncio, P., Creati, N., 2003. A lithospheric-scale seismogenic thrust in central Italy. J. Geodyn. 36/1-2, 79–94.

Liotta, D., 1996. Analisi del settore centro-meridionale del bacino Pliocenico di Radicofani (Toscana Meridionale). Boll. Soc. Geol. It. 115, 115–143.

Liotta, D., Salvatorini, G.F., 1994. Evoluzione sedimentaria e tettonica della parte centro-meridionale del bacino pliocenico di Radicofani. Studi Geologici Camerti vol. spec. 1, 65–78.

Lister, G.S., Davis, G.A., 1989. The origin of metamorphic core complexes and detachment faults formed during Tertiary continental extension in the northern Colorado River region, USA. J. Struct. Geol. 11, 65–93.

Mariucci, M.T., Muller, B., 2003. The tectonic regime in Italy inferred from borehole breakout data. Tectonophysics 361, 21–35.

Marson, I., Cernobori, L., Nicolich, R., Stoka, M., Liotta, D., Palmieri, F., Velicogna, I., 1998. CROP-03 profile: a geophysical analysis of data and results. Mem. Soc. Geol. It. 52, 123–137.

Melosh, H.J., 1990. Mechanical basis for low-angle normal faulting in the Basin and Range province. Nature 343, 331–335.

Miller, S.A., Collettini, C., Chiaraluce, L., Cocco, M., Barchi, M.R., Kaus, B., 2004. Aftershocks driven by a high pressure CO_2 source at depth. Nature 427, 724–727.

Minelli, G., 1992. Tectonic evolution of the Perugia Massif Area, Northern Apennines (Italy). PhD Thesis, Imperial College, London.

Mirabella, F., Ciaccio, M.G., Barchi, M.R., Merlini, S., 2004. The Gubbio normal fault (Central Italy): geometry, displacement distribution and tectonic evolution. J. Struct. Geol. 26, 2233–2249.

Mongelli, F., Zito, G., 1991. Flusso di calore nella regione Toscana. Studi Geologici Camerti 1, 91–98.

Montone, P., Amato, A., Pondrelli, S., 1999. Active stress map of Italy. J. Geophys. Res. 104B11, 25595–25610. doi:10.1029/1999JB900181.

Pascucci, V., Merlini, S., Martini, I.P., 1999. Seismic stratigraphy in the Miocene-Pleistocene sedimentary basins of the Northern Tyrrhenian Sea and western Tuscany (Italy). Basin Res. 11, 337–356.

Pauselli, C., Federico, C., 2002. The brittle/ductile transition along the Crop03 seismic profile: relationship with the geological features. Boll. Soc. Geol. It. 1, 25–35.

Peccerillo, A., 1985. Roman comagmatic province (central Italy): evidence for subduction-related magma genesis. Geology 13, 103–106.

Peccerillo, A., Panza, G., 1999. Upper mantle domains beneath central-southern Italy: petrological, geochemical and geophysical contraints. Pure Appl. Geophys. 156, 421–443.

Pialli, G., Barchi, M.R., Minelli, G., 1998. Results of the CROP03 deep seismic reflection profile. Memorie della Società Geologica Italiana 52, 657pp.

Piccinini, D., Cattaneo, M., Chiarabba, C., Chiaraluce, L., De Martin, M., Di Bona, M., Moretti, M., Selvaggi, G., Augliera, P., Spallarossa, D., Ferretti, G., Michelini, A., Govoni, A., Di Bartolomeo, P., Romanelli,

M., Fabbri, J.A., 2003. Microseismic study in a low seismicity area of Italy: the Città di Castello 2000–2001 experiment. Ann. Geophys. 46 (N6), 1315–1324.

Ponziani, F., De Franco, R., Minelli, G., Biella, G., Federico, C., Pialli, G., 1995. Crustal shortening and duplication of the Moho in the Northern Apennines: a view from seismic refraction data. Tectonophysics 252, 391–418.

Principi, G., Treves, B., 1984. Il sistema Corso-Appennino come prisma di accrezione. Riflessi sul problema generale del limite Alpi-Appennino. Mem. Soc. Geol. It. 28, 529–576.

Proffett, J.M., 1977. Cenozoic geology of the Yerington district, Nevada, and implications for the nature of Basin and Range faulting. Geol. Soc. Am. Bull. 88, 247–266.

Riguzzi, F., Tertulliani, A., Gasparini, C., 1989. Study of the seismic sequence of Porto San Giorgio (Marche), 3 July 1987. Il Nuovo Cimento 12, 453–467.

Rocchi, R., Westerman, S.D., Dini, A., Innocenti, F., Tonarini, S., 2002. Two-stage of laccoliths at Elba Island, Italy. Geology 30, 983–986.

Rutter, E.H., 1986. On nomenclature of mode of failure transitions in rocks. Tectonophysics 122, 381–387.

Saupé, F., Marignac, C., Moine, B., Sonet, J., Zimmerman, J.L., 1982. Datation par les mèthodes K/Ar et Rb/Sr de quelques roches de la partie orientale de l'ile d'Elbe Province de Livourne, Italie. Bulletin de Minéralogie 105, 236–245.

Selvaggi, G., Amato, A., 1992. Subcrustal earthquakes in the Northern Apennines (Italy): evidence for a still active subduction? Geophys. Res. Lett. 1921, 2127–2130.

Serri, G., Innocenti, F., Manetti, P., 1993. Geochemical and petrological evidence of the subduction of delaminated Adriatic continental litosphere in the genesis of the Neogene–Quaternary magmatism of central Italy. Tectonophysics 223, 117–147.

Sibson, R.H., 1985. A note on fault reactivation. J. Struct. Geol. 7, 751–754.

Suhadolc, P., Panza, G.F., 1989. Physical properties of the lithosphere–asthenosphere system in Europe from geophysical data. In: Boriani, A., Bonafede, M., Piccardo, G.B., Vai, G.B. (Eds.), The lithosphere in Italy Advanced Earth Science Researches Accademia Nazionale Of Lincei, Rome, 80, pp. 15–40.

Trevisan, L., 1950. L'Elba orientale e la sua tettonica di scivolamento per gravità. Memorie dell'Istituto Geologico dell'Università di Padova 16, 1–30.

Trevisan, L., Marinelli, G., Barberi, F., Giglia, G., Innocenti, F., Raggi, G., Squarci, P., Taffi, L., Ricci, C.A., 1967. Carta Geologica dell'Isola d'Elba. Scala 1:25,000. Consiglio Nazionale delle Ricerche, Gruppo di Ricerca per la Geologia dell'Appennino centro-settentrionale e della Toscana, Pisa.

Wernicke, B., 1995. Low-angle normal faults and seismicity: A review. J. Geophys. Res. 100, 20159–20174.

Wernicke, B., Axen, G.J., 1988. On the role of isostasy in the evolution of normal fault systems. Geology 16, 848–851.

Westaway, R., 1999. The mechanical feasibility of low-angle normal faulting. Tectonophysics 308, 407–443.

Yin, A., 1989. Origin of regional rooted low-angle normal faults: a mechanical model and its tectonic implications. Tectonics, 469–482.